KİMYA BİLİMİNDE DİSİPLİNLERARASI YAKLAŞIMLAR

Editör
FERDA ESER

BİDGE

BİDGE Yayınları

KİMYA BİLİMİNDE DİSİPLİNLERARASI YAKLAŞIMLAR

Editör: FERDA ESER

ISBN: 978-625-372-720-8

1. Baskı
Sayfa Düzeni: Gözde YÜCEL
Yayınlama Tarihi: 2025-06-25
BİDGE Yayınları

Sertifika No: 71374

www.bidgeyayinlari.com.tr - bidgeyayinlari@gmail.com
Krc Bilişim Ticaret ve Organizasyon Ltd. Şti.
Güzeltepe Mahallesi Abidin Daver Sokak Sefer Apartmanı No: 7/9 Çankaya / Ankara

ÖNSÖZ

Bilimsel bilginin hızla geliştiği günümüzde, farklı disiplinlerin kesişim noktalarında ortaya çıkan çalışmalar hem teorik bilgiyi hem de pratik uygulamaları derinlemesine anlamamıza olanak sağlamaktadır. Elinizdeki bu kitap, kimya, malzeme bilimi ve çevre alanlarında yürütülen çeşitli araştırmaları bir araya getirerek, güncel bilimsel konulara bütüncül bir bakış sunmayı amaçlamaktadır.

Her bölüm, ilgili alandaki kuramsal çerçeveyi sunmakla kalmayıp, aynı zamanda güncel literatür ışığında gelişmeleri ve geleceğe yönelik araştırma eğilimlerini de tartışmaktadır. Kitapta yer alan çalışmalar, hem temel bilimsel bilgiye katkı sunmakta hem de uygulama potansiyeli taşıyan alanlara ışık tutmaktadır.

Bu kitabın, okuyuculara faydalı bilgiler sunmasının yanı sıra, yeni fikirlerin filizlenmesine katkı sağlamasını umuyorum. Bilime ve araştırmaya gönül veren herkes için yararlı bir kaynak olması dileğiyle...

Prof. Dr. FERDA ESER

AMASYA ÜNİVERSİTESİ

İÇİNDEKİLER

BÖLÜM 1

TAŞ KÖMÜRÜ KATRANI BOYARMADDELERİ: TARİHSEL ÖNEMİ VE MODERN TEKSTİL UYGULAMALARINDAKİ ÇEVRESEL SORUNLAR

EMİNE BAKAN[1]

GİRİŞ

Boyarmaddelerin insanlık tarihindeki kullanımı, doğal kaynaklardan elde edilen pigmentlerle başlamış; ancak 19. yüzyılın ortalarından itibaren kimya bilimindeki gelişmeler sayesinde sentetik boyarmaddelere geçiş süreci hız kazanmıştır. Bu devrim niteliğindeki dönüşüm, özellikle taşkömürü katranından türetilen bileşiklerle mümkün olmuş ve modern kimya endüstrisinin temellerini atmıştır.

Taşkömürü katranı boyarmaddelerinin tarihsel gelişimi incelendiğinde, bu bileşiklerin ortaya çıkış sürecinin sistematik bilimsel yöntemlerden çok, dönemin sınırlı organik kimya bilgisiyle yürütülen deneysel ve çoğu zaman rastlantısal çalışmalara dayandığı görülmektedir. Özellikle 17. yüzyılda taşkömürü katranı gibi

[1] Dr. Öğr. Üyesi, Uşak Üniversitesi, Ulubey Meslek Yüksekokulu, Orcid: 0000-0002-3463-4314

kompleks organik karışımlarla ilgilenen ilk araştırmacılar, modern anlamda kimyasal analiz tekniklerinden yoksun olsalar da önemli gözlemler yapmışlardır. Bu bağlamda, 1648 yılında taşkömürünü damıtarak katran fraksiyonlarını izole eden ilk kimyagerlerden biri olarak kabul edilen Johan Rudolph Glauber, taşkömürü türevli maddelerin bilimsel incelemesine öncülük etmiştir. Tekstil boyamacılığında yaygın olarak kullanılan Glauber tuzu (sodyum sülfat) ile tanınan Glauber, yalnızca katkı maddesi düzeyinde değil, aynı zamanda katranın kimyasal potansiyelinin fark edilmesinde de öncü bir isimdir (İşmal, 2011).

1856 yılında William Henry Perkin'in taş kömürü katranındaki kimyasal yapının kinin ve anilin ile aynı olduğunu tespit etmesi, laboratuvar ortamında ilk sentetik boya *mauveine* nin sentezlenmesini sağlamıştır. Böylecce yalnızca tekstil endüstrisinde değil; aynı zamanda ilaç, gıda ve kozmetik gibi farklı sektörlerde de kimyasal ürünlerin seri üretimini mümkün kılan bir paradigma değişimini başlatmıştır (Beer, 1958).

Taşkömürü katranı, kok kömürü üretimi sırasında elde edilen kompleks bir yan ürün olup; aromatik hidrokarbonlar, fenoller, aminler ve heterosiklik bileşikler gibi çok sayıda organik maddeyi bünyesinde barındırır (Kim vd., 2019). Bu bileşiklerden sentezlenen boyarmaddeler —özellikle anilin türevleri, azo bileşikleri, antrakinon temelli yapılar ve trifenilmetan grubu boyalar— 19. ve 20. yüzyıllarda tekstil ürünlerinin boyanmasında yaygın olarak kullanılmıştır (Hunger, 2003). Renk skalasının genişliği, canlılık düzeyi ve düşük maliyet gibi avantajları, bu boyarmaddelerin hızla yayılmasını sağlamıştır. Azo, trifenilmetan, antrakinon ve indigoid grubu boyarmaddeler hem renk yelpazesinin genişliği hem de tekstil liflerine yüksek afinite göstermeleri nedeniyle 20. yüzyılın ortalarına kadar yoğun biçimde kullanılmıştır (Gregory, 2020).

Sentetik Boya Devrimi (Zaman Çizelgesi)

1856 – Mauveine (Perkin)

1862 – Anilin Kırmızısı

1878 – Azo boyalarının keşfi

1883 – Antrakinon türevleri

1900'ler – Endüstriyel ölçekte üretim

Zamanla taş kömürü katranı boyarmaddelerinin çevresel ve toksikolojik etkilerine dair bilimsel veriler artmış; bazı taşkömürü katranı türevlerinin genotoksik, mutajenik ve hatta karsinojenik etkilere sahip olduğu ortaya konmuştur (IARC, 2010; Yılmaz & Gökmen, 2020). Bu durum, Avrupa Birliği REACH düzenlemesi başta olmak üzere birçok uluslararası düzenlemenin devreye girmesine sebep olmuştur. Aynı zamanda çevresel sürdürülebilirlik açısından da bu maddelerin zor bozunabilir yapıları alternatif boyarmadde arayışlarını gündeme getirmiştir (Kant, 2012; Khandare & Govindwar, 2015; Wang vd., 2018).

Taşkömürü Katranı Boyarmaddelerinin Çevresel Döngüsü

Kaynaktan çıkış → tekstile uygulanış → atık su → arıtma tesisi → çevresel deşarj

Günümüzde birçok ülke, taşkömürü katranı türevli boyarmaddelerin kullanımını ciddi şekilde sınırlamış veya tamamen yasaklamıştır. Avrupa Birliği'nin REACH yönetmeliği kapsamında, 22'den fazla azo boyarmadde doğrudan tekstil ve deri ürünlerinde yasaklanmıştır (ECHA, 2023). Türkiye'de de TS EN ISO 14362-1 standardı kapsamında boyanmış ürünlerde yasaklı azo boyaların analizine ilişkin zorunluluklar getirilmiştir.

Bu kapsamda bu kitap bölümü, taşkömürü katranı kaynaklı boyarmaddelerin tarihsel gelişimini, kimyasal yapılarını, toksikolojik etkilerini ve çevresel risklerini bütüncül bir yaklaşımla

değerlendirmeyi amaçlamaktadır. Ayrıca modern tekstil endüstrisinde sürdürülebilirlik ekseninde bu boyarmaddelerin güncel rolü, yerini almakta olan alternatif teknolojiler ve geleceğe yönelik bilimsel yaklaşımlar da detaylı biçimde analiz edilecektir.

TAŞKÖMÜRÜ KATRANI BOYARMADDELERİNİN TARİHÇESİ

Sentetik boyarmadde endüstrisinin başlangıcı, kimya tarihinde bir dönüm noktası olarak kabul edilir. Bu sürecin temelinde, taşkömürü katranından elde edilen kimyasal bileşikler yer alır. Taşkömürü katranı, kok kömürü üretimi sırasında elde edilen yoğun aromatik bileşikler içeren siyah renkli bir yan üründür ve modern boya kimyasının hammaddesi olarak 19. yüzyıl ortalarında dikkat çekmeye başlamıştır (Hunger, 2003; Travis, 1993).

Mauveine'in Keşfi ve Anilin Devrimi

1856 yılında İngiliz kimyager William Henry Perkin, kininden kinin sentezi yapmaya çalışırken tesadüfen *mauveine* adlı ilk sentetik boyarmaddeyi elde etti. Bu olay, organik boyarmadde endüstrisinin doğuşuna zemin hazırlamış, aynı zamanda katran kökenli bileşiklerin boyar özelliklerinin keşfine kapı aralamıştır (Garfield, 2001). Mauveine, o dönemin doğal mor boyarmaddelerine göre çok daha canlı ve dayanıklıydı. Üstelik endüstriyel ölçekte üretimi mümkündü. Bu özellikleri, sentetik boyaların tekstil endüstrisinde hızla benimsenmesine neden oldu.

19. Yüzyıl Sonları: Boya Kimyasının Sanayileşmesi

Mauveine'in ticari başarısı kısa sürede Avrupa kıtasına yayıldı. Almanya, bu alandaki kimyasal bilgi birikimini hızla üretime dönüştürdü. BASF, Bayer, Hoechst ve AGFA gibi kimya şirketleri, taşkömürü katranından anilin, fenol, naftalin gibi türevleri izole ederek azo, trifenilmetan ve antrakinon boyarmadde sınıflarını geliştirdi (Gregory, 2020). 1862'de anilin kırmızısı (fuksin), 1869'da

ilk sentetik alizarin (antrakinon grubu), 1878'de ilk azo boyası (Bismarck Brown) üretildi. Bu dönem, Almanya'nın "anilin boyası krallığı" olarak anılmasına neden olmuştur. Kimya endüstrisinin devlet destekli Ar-Ge anlayışı ve üniversite-sanayi iş birliği sayesinde, 1900'lü yıllara gelindiğinde yüzlerce taşkömürü katranı türevli boyarmadde uluslararası pazarda yer almaya başlamıştır (Hunger, 2003).

20. Yüzyıl Başlarında Kullanımın Yaygınlaşması

Sentetik boyarmaddelerin, doğal boyalara göre çok daha ucuz ve stabil olması, kısa sürede küresel tekstil pazarında standart haline gelmesini sağladı. Yün, pamuk, ipek ve sentetik liflerin boyanmasında farklı gruplardan boyarmaddeler kullanıldı. Özellikle askeri tekstiller, okul üniformaları ve ev tekstilinde bu boyalar tercih edildi. Ayrıca, bu dönemde kozmetik, matbaa, deri ve gıda sektörlerinde de taşkömürü türevli boyarmaddelerin kullanımı arttı (Shore, 2002).

Toksikolojik Bulgular ve İlk Sınırlamalar

Ancak 20. yüzyılın ortalarına gelindiğinde, bu boyarmaddelerin bir kısmının toksik ve karsinojenik özellikler taşıdığına ilişkin bilimsel çalışmalar yayımlanmaya başlandı. Aromatik amin yapılarının, insan vücudunda biyotransformasyonla kansere neden olabilecek bileşiklere dönüştüğü gösterildi (IARC, 2010). Özellikle tekstil işçilerinde ve saç boyası kullanıcılarında mesane kanseri vakalarındaki artış, boyarmadde kullanımındaki düzenlemelerin gündeme gelmesine neden oldu.

Günümüz: Yasaklar ve Alternatif Arayışlar

Günümüzde taşkömürü katranı türevli birçok boyarmadde, Avrupa Birliği başta olmak üzere birçok ülkede kullanım açısından ciddi kısıtlamalara tabi tutulmuştur. Avrupa Birliği REACH mevzuatı çerçevesinde tekstil ve deri ürünlerinde kullanımı

yasaklanan azo boyarmadde sayısı 22'ye ulaşmıştır (ECHA, 2023). Türkiye'de de bu düzenlemeler TS EN ISO 14362-1 standardı ile ulusal mevzuata entegre edilmiştir (TS EN ISO 14362-1, 2023).

Bununla birlikte, bu boyarmaddelerin tarihsel önemi ve kimya endüstrisinin gelişimindeki merkezi rolü göz ardı edilemez. Bugün sürdürülebilir alternatifler geliştirilirken, taşkömürü katranı boyarmaddelerinin kimyasal yapıları hâlâ birçok yeni molekülün tasarımında referans niteliği taşımaktadır.

KİMYASAL YAPILAR VE MOLEKÜLER ÖZELLİKLER

Taşkömürü katranı boyarmaddeleri, kökenini aromatik hidrokarbonlar, aminler, fenoller ve heterosiklik bileşikler gibi bileşenlerden alan organik boyarmaddelerdir. Bu maddeler, yapı bakımından oldukça kompleks olmakla birlikte, belirli sınıflara ayrılarak kimyasal olarak kategorize edilebilir. Renk veren özellikler, konjugasyon sistemleri, elektron çekici/itici grupların yapıya katılması ve azo bağları gibi fonksiyonel gruplar aracılığıyla kazanılır (Zollinger, 2003).

Taşkömürü Katranının Kimyasal Bileşenleri

Taşkömürü katranı, yaklaşık %70'ten fazlası aromatik hidrokarbonlar olmak üzere yüzlerce organik bileşen içerir. Başlıca bileşen grupları:

Naftalin türevleri

Fenol ve krezoler

Anilin ve türevleri

Heterosiklik bileşikler (piridin, kinolin, karbazol)

Bu bileşenler, uygun reaksiyon koşullarında nitrolama, sülfanasyon, diazotasyon gibi klasik organik sentez yöntemleri ile boyarmadde üretiminde kullanılır (Kim vd., 2019).

Başlıca Boyarmadde Sınıfları

Azo Boyarmaddeleri

Yapılarında -N=N- azo grubu içerirler.

Genellikle anilin türevlerinden diazotasyon reaksiyonuyla sentezlenir.

Geniş bir renk yelpazesi sunar; özellikle sarı, kırmızı ve turuncu tonlarda.

Antrakinon Boyarmaddeleri

Antrakinon iskeleti ($C_{14}H_8O_2$) üzerine çeşitli elektron çekici/itici grupların eklenmesiyle renklilik kazanır.

Mavi ve mor tonlarda mükemmel ışık haslığı sağlar.

Alizarin gibi doğal boyaların sentetik eşdeğeridir.

Trifenilmetan Boyarmaddeleri

Renkli katyonik yapılar içerir.

Parlak mor, mavi ve yeşil tonlarda kullanılır.

Tekstil dışında mürekkep, boya ve gösterge maddesi olarak da kullanılır.

Indigoid ve Oksazin Boyarmaddeleri

Daha özel ve nadir yapılar olmakla birlikte, yüksek renk haslıkları ve kendine özgü renkler üretirler.

Özellikle denim üretiminde kullanılan indigo boyası bu gruptadır.

Renklenme Mekanizması ve Elektronik Geçişler

Boyarmaddelerin renk göstermesi, yapılarındaki konjuge π bağ sistemleri sayesinde görünür ışık spektrumundaki bazı dalga boylarını absorplamalarına bağlıdır. Azo, karbonil, hidroksil gibi

gruplar, bu konjuge sistemin genişliğini ve dolayısıyla ışığın hangi kısmını absorplayacağını belirler (Zollinger, 2003). Elektron çekici ve verici grupların yapıya katılması, bathochromic (kırmızıya kayma) veya hypsochromic (maviye kayma) etkiler yaratır.

Liflerle Etkileşim ve Bağlanma Mekanizmaları

Taşkömürü katranı boyarmaddeleri, lif türüne göre farklı bağlanma mekanizmaları gösterir:

Pamuk (selülozik lifler): Direkt ve reaktif boyarmaddeler hidrojen bağları ve van der Waals etkileşimleriyle bağlanır.

Yün ve ipek (protein lifleri): Asidik boyarmaddeler iyonik bağlarla bağlanır.

Sentetik lifler (poliester, akrilik): Dispers boyarmaddeler hidrofobik etkileşimlerle lif içine difüze olur.

Boyarmadde molekülünün büyüklüğü, polaritesi ve çözünürlük parametreleri, lifle etkileşim kabiliyetini doğrudan etkiler (Shore, 2002).

TEKSTİL ENDÜSTRİSİNDEKİ UYGULAMALARI

Taşkömürü katranı kaynaklı sentetik boyarmaddeler, 19. yüzyılın ikinci yarısından itibaren tekstil endüstrisinde doğal boyarmaddelere alternatif olarak hızla yaygınlaşmıştır. Renk yelpazelerinin genişliği, üretim maliyetlerinin düşüklüğü ve uygulama kolaylıkları, bu boyarmaddelerin özellikle endüstriyel ölçekte tercih edilmesini sağlamıştır (Tonogai ve ark., 1979).

Lif Türlerine Göre Uygulama Alanları

Taşkömürü katranı türevli boyarmaddeler, hem doğal hem de sentetik lif türlerine uygun çeşitli boyama sınıflarına ayrılarak kullanılmıştır:

Pamuk (selülozik lifler): Direkt boyarmaddeler (örneğin, Congo Red), selüloz liflerine doğrudan bağlanabilir. Reaktif olmayan ancak geniş konjugasyon yapıları sayesinde fiziksel adsorpsiyonla tutunurlar.

Yün ve ipek (protein lifleri): Asidik boyarmaddeler, amino gruplar ile iyonik bağlar kurarak liflere güçlü biçimde bağlanır. Azo ve trifenilmetan grubu asidik boyalar, bu lifler üzerinde yüksek renk canlılığı sağlar.

Polyester ve akrilik (sentetik lifler): Dispers boyarmaddeler, düşük molekül ağırlıkları ve hidrofobik özellikleri sayesinde bu liflere ısı ve basınç altında difüze olur. Özellikle antrakinon türevleri bu liflerle iyi uyum sağlar.

Boyama Yöntemleri ve Uygulama Teknikleri

Direkt boyama: Su içerisinde çözünmüş boyarmadde doğrudan lifle temas ettirilir; pamuklu tekstillerde yaygındır.

Asidik boyama: Asidik pH altında yürütülen bu yöntem özellikle yün ve ipek için uygundur. Azo grubu içeren boyalar sıklıkla kullanılır.

Dispers boyama: Suya düşük çözünürlüğe sahip boyarmaddeler yüksek sıcaklıkta lif içerisine nüfuz ettirilir. Polyester kumaşlar için ideal yöntemdir.

Performans Özellikleri

Taşkömürü katranı türevli boyarmaddelerin performans düzeyleri, hem kimyasal yapıya hem de lif tipiyle olan etkileşime bağlıdır. Tablo 1’de performans özellikleri verilmiştir.

Tablo 1. *Taşkömürü katranı boyarmaddelerin performans özellikleri*

Performans Özelliği	Açıklama
Renk haslığı	Işık, yıkama, sürtünme ve ter gibi etkenlere karşı dayanıklılık; antrakinon ve azo boyalar genellikle yüksek haslık gösterir.
Renk yoğunluğu	Geniş konjugasyon sistemleri nedeniyle canlı ve doygun renkler elde edilebilir.
Çözünürlük ve migrasyon	Özellikle düşük moleküler ağırlıklı boyalar yüksek mobilite gösterebilir; bu da liften ayrılma riskini artırır.

Tablo 2. *Lif Tipine Göre Uygun Boyarmadde Grupları*

Lif Tipi	Uygun Boyarmadde Grubu	Uygulama Yöntemi
Pamuk	Direkt, reaktif	Pad-batch, exhaust
Yün	Asidik	Acid dyeing
İpek	Asidik	Dip-dyeing
Polyester	Dispers	High temperature HT
Akrilik	Katyonik, dispers	Pressure dyeing

Uygulama Alanları

Taşkömürü katranı boyarmaddeleri, sadece giyim ürünlerinde değil aynı zamanda teknik tekstillerde de önemli bir rol oynamıştır:

Giyim ve moda tekstilleri: Renk çeşitliliği sayesinde tişört, elbise, dış giyim ürünlerinde geniş kullanım alanı buldu.

Askeri tekstiller: Kamuflaj kumaşlarında kullanılan koyu yeşil, kahverengi, siyah tonlar sıklıkla azo/antrakinon boyalarla elde edilmiştir.

Ev tekstilleri: Perde, döşemelik kumaş, halı gibi ürünlerde yüksek renk haslığı tercih edilmiştir.

Sanayi tekstilleri: Taşkömürü boyaları, filtre bezleri, teknik örtüler gibi ürünlerde uygulandı.

TOKSİKOLOJİK ETKİLER VE İNSAN SAĞLIĞI ÜZERİNDEKİ RİSKLER

Taşkömürü katranı türevli boyarmaddeler, aromatik yapıları ve kimyasal stabiliteleri nedeniyle tekstil endüstrisinde yaygın biçimde kullanılmıştır. Ancak bu yapısal özellikler aynı zamanda insan sağlığı açısından potansiyel toksisite risklerini de beraberinde getirmiştir. Özellikle bazı azo boyarmaddeleri ve aromatik amin türevleri, genotoksik, mutajenik ve karsinojenik etki gösterme potansiyelleri nedeniyle dikkatle incelenmektedir (IARC, 2010; Yılmaz & Gökmen, 2020).

Aromatik Aminler ve Karsinojenite Riski

Birçok taşkömürü katranı türevli boya, yapısında anilin, benzidin, toluidin, naftilamin gibi aromatik aminleri doğrudan veya dolaylı biçimde barındırır. Azo boyarmaddeler, özellikle anaerobik metabolik koşullarda (örneğin insan karaciğeri, cilt mikroflorası) azo bağlarının (-N=N-) indirgenmesiyle aromatik aminlere dönüşebilir. Bu aminlerin bazıları mesane kanseriyle doğrudan ilişkilendirilmiştir (IARC, 2010). Örneğin *Benzidin* türevli boyalar (Direct Black 38, Direct Blue 6) yüksek düzeyde karsinojeniktir ve birçok ülkede yasaklanmıştır.

Uluslararası Toksikoloji Sınıflandırmaları

IARC (International Agency for Research on Cancer) (IARC, 2010): Azo boyarmaddeler arasında bazıları Grup 1 (İnsan için kanıtlanmış karsinojen) sınıfına alınmıştır. Benzidin, 2-naftilamin, 4-aminobifenil gibi bileşikler bu gruptadır.

ECHA – REACH Ek XVII (ECHA, 2023): AB'de, tüketiciyle temas eden tekstil ve deri ürünlerinde kullanılmak üzere 22 azo

boyarmadde yasaklanmıştır. Yasaklı aminler arasında o-anisidin, 4-kloroanilin, 2,4-toluenediamin gibi yapılar yer alır.

EPA – TSCA (ABD) (EPA, 2023): Azo boyarmaddeler ve bileşenleri, *high concern* kimyasallar listesinde izlenmektedir. Bazı boyarmaddelere yönelik *Significant New Use Rules (SNUR)* yayınlanmıştır.

Maruziyet Yolları ve Risk Grupları

İş yeri maruziyeti: Tekstil işçileri, özellikle boyama, kesim ve ütüleme birimlerinde aerosol, toz veya cilt teması yoluyla maruz kalabilirler. Bu gruplarda deri iritasyonları, kontakt dermatit ve solunum yolu semptomları bildirilmiştir.

Kullanıcı maruziyeti: Boyanmış tekstil ürünlerinin uzun süreli cilt teması (örneğin iç giyim, çocuk kıyafetleri), özellikle vücut sıcaklığı ve ter ile temas halinde boyarmaddenin liften ayrılması ve deri yoluyla emilimi ile sonuçlanabilir.

Kozmetik ve saç boyaları: Taşkömürü türevli bazı bileşikler, saç boyalarında da geçmişte yaygın olarak kullanılmış ve mesane kanseri ile ilişkilendirilmiştir (Bolt & Golka, 2012).

Bilimsel Bulgular ve Vaka Çalışmaları

Yılmaz & Gökmen (2020): Azo boyarmaddelerin toksikolojik etkilerini değerlendirmiş; bazı boyaların DNA hasarı, oksidatif stres ve enzim inhibisyonu yaptığı belirlenmiştir.

Kant (2012): Tekstil boyalarının atık sularla çevreye yayılmasının ekotoksik etkilerini vurgular; bu etkiler insan sağlığına dolaylı yollardan (su, gıda zinciri) ulaşabilir.

Toksikolojik riskler yalnızca kullanılan boya miktarıyla değil, aynı zamanda boya maddesinin moleküler yapısı, lifle bağlanma gücü, çevresel koşullar (pH, sıcaklık, enzimatik faaliyet)

gibi faktörlerle doğrudan ilişkilidir. Bu nedenle risk değerlendirmelerinde çok boyutlu bir yaklaşım gereklidir.

ÇEVRESEL ETKİLER

Taşkömürü katranı kökenli boyarmaddeler, kimyasal stabilite, yüksek molekül ağırlığı ve geniş konjuge π-sistemleri gibi yapısal özellikleri nedeniyle çevresel açıdan "kalıcı organik kirleticiler" (Persistent Organic Pollutants - POPs) kategorisine yakın davranışlar sergileyebilirler. Özellikle azo ve antrakinon grubu boyarmaddeler, atık sular aracılığıyla su ve toprak ekosistemlerine taşınmakta, çevre sağlığı açısından ciddi tehditler oluşturmaktadır (Wang vd., 2018; Kant, 2012).

Atık Su Kirliliği ve Renklenme Sorunu

Boyarmaddelerin çevreye en yoğun salınımı tekstil fabrikalarının boyama işlemi sonrası ortaya çıkan atık suları aracılığıyla gerçekleşir. Bu sular genellikle; yüksek renk yoğunluğuna sahip, zayıf biyobozunurluk gösteren,toksite içeriği yüksek karakterdedir.

Birçok boyarmadde, konvansiyonel atık su arıtma sistemlerinde parçalanmadan kalır ve doğal su kaynaklarında renkli, toksik kalıntılar oluşturur (Khandare & Govindwar, 2015).

Biyobozunabilirlik ve Kalıcılık Sorunları

Boyarmaddelerin kimyasal yapısı çevresel bozunabilirliklerini doğrudan etkiler [Tablo 3].

Tablo 3. *Boyarmaddelerin Bozunma Süreçleri*

Boyarmadde Grubu	Bozunma Durumu	Çevresel Kalıcılık
Azo boyalar	Redüktif şartlarda parçalanabilir (amin üretir)	Orta–yüksek
Antrakinon boyalar	Yüksek stabilite (aromatik halka sistemi)	Yüksek
Trifenilmetan	Yüksek renk yoğunluğu, bozunması zor	Yüksek

Özellikle antrakinon ve trifenilmetan grubu boyarmaddeler, UV, ozon, biyolojik arıtım gibi yöntemlere karşı direnç gösterir.

Ekotoksisite: Su Canlılarına ve Mikroorganizmalara Etkileri

Araştırmalar, taşkömürü katranı boyarmaddelerinin birçok tatlı su organizması üzerinde toksik, mutajenik ve genotoksik etkiler oluşturduğunu göstermektedir. Özellikle; Alg gelişimini baskılama, balıkların solungaç ve karaciğer dokusunda yapısal hasar, su mikroflorası üzerinde enzimatik inhibisyon gözlenmiştir (Yılmaz & Gökmen, 2020; Wang vd., 2018).

Ayrıca bu maddelerin çevrede uzun süre kalması, biyomagnifikasyon riski yaratmakta; yani besin zinciri aracılığıyla birikerek insanlara kadar ulaşabilmektedir.

Toprak ve Tarım Üzerindeki Dolaylı Etkiler

Arıtılmadan salınan tekstil atık suları zamanla tarımsal alanlara taşınabilir. Bu durum; Toprak mikrobiyal dengesini bozabilir, ağır metal ve toksik kalıntılarla toprak verimliliğini düşürebilir, tarım ürünlerinde kontaminasyon riski doğurabilir (Kant, 2012).

Çevre Dostu Arıtma Yöntemleri ve Mevcut Sorunlar

Çevresel etkileri azaltmak için çeşitli teknikler geliştirilmektedir [Tablo 4].

Tablo 4. *Boyarmaddenin çevresel etkilerinin azaltılması için yöntemler*

Yöntem	Açıklama	Avantaj / Sınırlama
Ozon oksidasyonu	Ozon gazı ile yapısal yıkım	Yüksek maliyet
Gelişmiş fotooksidasyon	UV + H_2O_2 kombinasyonu	Bazı boyalara etkisiz
Mikrobiyal arıtım	Enzim veya bakteri temelli yıkım	Yavaş süreç, selektivite sorunları
Membran filtrasyon	Nanofiltrasyon, ters ozmoz	Enerji ihtiyacı yüksek

Tüm bu yöntemler, farklı koşullarda sınırlı başarı sağlamaktadır ve genellikle çok bileşenli boyarmadde karışımlarına karşı yetersiz kalmaktadır (Khandare & Govindwar, 2015).

Taşkömürü katranı boyarmaddelerinin çevresel etkileri, yalnızca fiziksel renk kirliliğinden ibaret değildir. Bu maddeler ekosistem sağlığı, halk sağlığı ve tarım sistemi üzerinde çok boyutlu ve kalıcı tehditler oluşturmaktadır. Bu nedenle sürdürülebilir tekstil üretiminde bu bileşiklerin kullanımının sınırlandırılması, alternatif yeşil çözümlerin önceliklendirilmesi gereklidir.

DÜZENLEME VE YASAKLAMALAR

Taşkömürü katranı kökenli sentetik boyarmaddeler, özellikle 20. yüzyılın ortalarından itibaren toksikolojik verilerin artmasıyla birlikte çeşitli yasal düzenlemelere, sınırlamalara ve yasaklamalara tabi tutulmuştur. Bu boyarmaddelerin özellikle azo grubu taşıyan türleri, sağlık ve çevre açısından yüksek risk taşıdıkları gerekçesiyle pek çok ülkenin kimyasal güvenlik mevzuatında yer almaktadır (ECHA, 2023; EPA, 2023).

Avrupa Birliği (AB) – REACH Yönetmeliği ve Ek XVII

AB'nin kimyasal maddelerin üretim ve kullanımını düzenleyen REACH (Registration, Evaluation, Authorisation and Restriction of Chemicals) yönetmeliği kapsamında, Ek XVII

listesinde yer alan birçok boyarmadde, tekstil ve deri ürünlerinde kullanım açısından yasaklanmıştır.

Kısıtlama kapsamı: Tüketiciyle doğrudan temas eden tekstil, deri, halı, giysi gibi ürünlerde 30 ppm'nin üzerinde 22 adet aromatik amin oluşturabilecek azo boyarmaddenin kullanımı yasaktır.

Sıklıkla yasaklanan bileşikler: Benzidin, 4-aminobifenil, 2-naftilamin, o-anisidin gibi yapılar.

Test standardı: TS EN ISO 14362-1 / 14362-3 test yöntemleri kullanılarak tekstil ürünlerinde bu boyaların analizi zorunludur.

Amerika Birleşik Devletleri – TSCA ve FDA Düzenlemeleri

ABD'de boyarmaddelerin yönetimi, Toxic Substances Control Act (TSCA) kapsamında EPA tarafından yürütülür. TSCA kapsamında:

SNUR (Significant New Use Rules): Belirli boyarmaddeler için yeni kullanım bildirim zorunluluğu getirilmiştir.

FDA: Gıda ile temas eden ambalajlarda ve kozmetikte kullanılan bazı katran türevli boyalar tamamen yasaklanmıştır (FDA, 2023).

Saç boyaları: Katran kökenli maddelerin kullanımına dair uyarı etiketlemesi zorunludur (örneğin "This product contains ingredients known to the State of California to cause cancer").

Türkiye – Kimyasalların Envanteri ve Kontrolü Yönetmeliği

Türkiye, REACH sistemine büyük ölçüde uyum sağlamış durumdadır.

Çevre, Şehircilik ve İklim Değişikliği Bakanlığı tarafından yürütülen Kimyasalların Envanteri ve Kontrolü Yönetmeliği kapsamında azo boyarmaddelere ilişkin REACH esasları geçerlidir. Tekstil ürünlerinde, TS EN ISO 14362-1 standardı ile yasaklı amin

oluşturan azo boyarmaddelerin test edilmesi yasal bir zorunluluktur. Ayrıca belirli boyarmaddeler "zararlı kimyasal" statüsünde sınıflandırılarak KKS (Kimyasal Kayıt Sistemi) üzerinden kayıt altına alınır.

Uluslararası Sertifikasyon ve Etiketleme Sistemleri

Düzenlemelerin yanı sıra tekstil ürünlerinin insan sağlığına zarar vermeyeceğini belgeleyen çeşitli sertifikasyon sistemleri geliştirilmiştir:

OEKO-TEX® Standard 100: Tekstil ürünlerinin azo boyarmadde ve ağır metal içeriği açısından güvenli olduğunu belgeleyen uluslararası sistem. Belirli aminleri oluşturabilecek boyarmaddelerin kullanımı yasaktır (OEKO-TEX®, 2023).

GOTS (Global Organic Textile Standard): Organik tekstillerde toksik kimyasalların kullanılmamasını şart koşar (Standard, G. O. T., 2010).

Düzenleyici kurumlar, bilimsel toksikoloji verilerine dayanarak taşkömürü katranı kökenli birçok boyarmaddeyi yasaklamış veya ciddi biçimde sınırlamıştır. Günümüzde, sürdürülebilir üretim hedefleri doğrultusunda sadece yasal zorunluluklar değil; aynı zamanda gönüllü sertifikasyon sistemleri ve kurumsal çevre politikaları da bu boyarmaddelerin kullanımını azaltma yönünde güçlü bir etki oluşturmaktadır.

SÜRDÜRÜLEBİLİRLİK PERSPEKTİFİ VE GELECEK ÖNERİLER

Taşkömürü katranı kökenli sentetik boyarmaddeler, tarihsel olarak tekstil endüstrisinde devrimsel nitelikte bir dönüşüm sağlamış; renk yelpazesi, ekonomik üretim kapasitesi ve teknik performans açısından geniş bir uygulama alanı bulmuştur. Ancak bu boyarmaddelerin toksikolojik, çevresel ve kalıcılık odaklı etkileri, günümüzün sürdürülebilirlik anlayışıyla önemli bir çatışma

içindedir. Bu nedenle bu tür sentetik boyaların günümüzdeki rolü yalnızca kimyasal performans açısından değil; aynı zamanda çevresel etki, insan sağlığı ve etik üretim bağlamında yeniden değerlendirilmelidir.

Sürdürülebilir Tekstil Üretimi Bağlamında Değerlendirme

Sürdürülebilirlik; yalnızca doğal kaynak kullanımını azaltmak değil, aynı zamanda toksik kimyasalların kullanımını sınırlandırmak, atık yönetimini iyileştirmek ve insan sağlığını önceleyen üretim süreçleri geliştirmek anlamına gelir.

Taşkömürü katranı türevli boyarmaddeler bu açıdan değerlendirildiğinde; sürdürülebilir hammaddelere dayanmamaktadır, yüksek toksik potansiyel taşımaktadır, zor bozunabilirliği nedeniyle çevrede uzun süre kalıcıdır, atık su yönetimini karmaşıklaştırmaktadır. Dolayısıyla bu boyarmaddelerin günümüz sürdürülebilir tekstil hedefleriyle uyumsuz olduğu açıkça ortadadır.

Alternatif Boyarmadde Arayışları

Doğal Boyarmaddeler: Bitki, mantar, böcek ve mikroorganizmalar kaynaklı pigmentler. Genellikle biyoçözünür ve toksik olmayan yapıdadırlar.

Dezavantajları: Renk haslığı düşüklüğü, sınırlı renk yelpazesi, standardizasyon sorunları.

Biyoteknolojik Boyarmaddeler : Mikrobiyal pigmentler (örneğin *Monascus*, *Streptomyces*, *Fusarium* türlerinden elde edilen renkler). Fermente üretimle düşük enerji tüketimi sağlarlar. Gelişmekte olan bir alan olup teknik optimizasyona ihtiyaç vardır.

Yeşil Kimya Tabanlı Sentetik Boyalar: Aromatik amin içermeyen, düşük toksisiteli, su bazlı sentetik sistemler. Sürdürülebilir liflerle

(TENCEL™, organik pamuk, geri dönüştürülmüş polyester) uyumlu üretim senaryoları oluşturabilirler.

Sertifikasyon ve Tüketici Bilinci

Sürdürülebilir üretimin yalnızca teknik değil; aynı zamanda etik ve şeffaf bir yaklaşım gerektirdiği kabul edilmektedir. Bu bağlamda ; OEKO-TEX®, GOTS, bluesign® gibi sistemler yalnızca üretim aşamasını değil, hammaddeden nihai ürüne kadar tüm süreci denetler. Tüketici düzeyinde artan bilinç, markaları çevre dostu etiketlemeye ve alternatif boyarmadde kullanımına teşvik etmektedir.

SONUÇ

Taşkömürü katranı kökenli boyarmaddeler, modern kimya ve tekstil endüstrisinin gelişiminde belirleyici bir rol oynamış; 19. yüzyıldan itibaren sentetik boya teknolojisinin temellerini atmıştır. Bu boyarmaddeler, gerek ekonomik gerekse teknik performans açısından uzun yıllar boyunca tekstil üretiminin vazgeçilmez unsurları arasında yer almıştır. Ancak zaman içinde bu maddelerin toksikolojik etkileri, çevresel kalıcılığı ve insan sağlığına yönelik olası zararları daha net biçimde anlaşılmış; böylece birçok ülke ve uluslararası kuruluş tarafından ciddi biçimde düzenlemeye tabi tutulmuştur.

Bu çalışmada, taşkömürü katranı boyarmaddelerinin tarihsel gelişimi, kimyasal yapıları, tekstil endüstrisindeki uygulamaları, toksikolojik etkileri ve çevresel riskleri detaylı bir şekilde incelenmiştir. Ayrıca mevcut yasal düzenlemeler değerlendirilmiş ve sürdürülebilirlik perspektifi çerçevesinde alternatif arayışlara yer verilmiştir. Elde edilen bulgular ışığında şu temel çıkarımlar yapılabilir:

Tarihsel mirasları güçlü olsa da, taşkömürü katranı boyarmaddeleri günümüz çevre ve insan sağlığı standartlarıyla örtüşmemektedir.

Azo ve aromatik amin türevli boyarmaddeler, hem insan sağlığı hem de sucul ekosistemler açısından yüksek risk taşıyan yapılar arasında yer almaktadır.

Düzenlemeler, bu boyarmaddelerin tekstil ve deri ürünlerinde kullanımını sınırlandırmış; ancak gelişmekte olan ülkelerde denetim eksiklikleri uygulamada farklılık yaratmaktadır.

Sürdürülebilir alternatifler, doğal boyarmaddeler, biyoteknolojik pigmentler ve düşük toksisiteli yeni sentetik sistemler aracılığıyla geliştirilmeye başlanmıştır.

Gelecek çalışmalar, döngüsel ekonomi ilkelerine dayalı boyama sistemleri, toksikolojik riski düşük pigmentler ve doğa dostu proses geliştirme üzerine yoğunlaşmalıdır.

Sonuç olarak, taşkömürü katranı boyarmaddeleri, kimya ve tekstil endüstrilerinin evriminde önemli bir dönemi temsil etmektedir. Ancak sürdürülebilirlik odaklı bir gelecek vizyonu doğrultusunda bu tür maddelerin yerini daha çevre dostu, biyolojik uyumlu ve sorumlu üretim anlayışını benimseyen alternatiflere bırakması kaçınılmazdır. Bu geçiş süreci yalnızca bilimsel değil; aynı zamanda etik, yasal ve toplumsal boyutlarıyla da yönetilmesi gereken çok katmanlı bir dönüşümdür.

KAYNAKÇA

Beer, J. J. (1958). Coal tar dye manufacture and the origins of the modern industrial research laboratory. *Isis*, *49*(2), 123-131.

Bolt, H. M., & Golka, K. (2012). The debate on carcinogenicity of hair dyes: New insights. Critical Reviews in Toxicology, 42(2), 101–103.

ECHA. (2023). Substances restricted under REACH. European Chemicals Agency. https://echa.europa.eu/substances-restricted-under-reach

EPA. (2023). Toxic Substances Control Act (TSCA) Chemical Substance Inventory. United States Environmental Protection Agency. https://www.epa.gov/tsca-inventory

FDA. (2023). Cosmetic Labeling Regulations. U.S. Food and Drug Administration. https://www.fda.gov/cosmetics/cosmetics-labeling-regulations

Garfield, S. (2001). Mauve: How one man invented a colour that changed the world. Faber and Faber.

Gregory, P. (2020). The current status of synthetic organic dyes in textiles. Coloration Technology, 136(3), 203–213.

Hunger, K. (2003). Industrial dyes: Chemistry, properties, applications. Wiley-VCH.

IARC. (2010). Some aromatic amines, organic dyes, and related exposures (Vol. 99). International Agency for Research on Cancer. https://publications.iarc.fr/Book-And-Report-Series/Iarc-Monographs-On-The-Identification-Of-Carcinogenic-Hazards-To-Humans/Some-Aromatic-Amines-Organic-Dyes-And-Related-Exposures-2010

İşmal, Ö. E. (2011). Boyarmadde Endüstrisinin Öncüsü: bir bilim adamı ve entelektüel olarak Sir WILLIAM HENRY PERKIN. *Yedi*, (6), 23-30.

Kant, R. (2012). Textile dyeing industry: An environmental hazard. Natural Science, 4(1), 22–26.

Khandare, R. V., & Govindwar, S. P. (2015). Phytoremediation of textile dyes and effluents: Current scenario and future prospects. Biotechnology Advances, 33(8), 1697–1714.

Kim, Y. J., Kim, K. H., & Jeon, E. C. (2019). Comprehensive characterization of chemical constituents in coal tar using GC × GC–TOFMS. *Analytical Methods*, 11(4), 475–483.

OEKO-TEX®. (2023). STANDARD 100 by OEKO-TEX®: Test criteria and limit values. https://www.oeko-tex.com/en/our-standards/standard-100-by-oeko-tex

Shore, J. (2002). Colorants and auxiliaries: Volume 1: Colorants (2nd ed.). Society of Dyers and Colourists.

Standard, G. O. T. (2010). GOTs. *Retrieved 15.06.2025*.

Tonogai, Y., Ito, Y., Iwaida, M., Tati, M., Ose, Y., & Sato, T. (1979). Studies on the toxicity of coal-tar dyes II. Examination of the biological reaction of coal-tar dyes to vital body. *The Journal of Toxicological Sciences*, *4*(3), 211-219.

Travis, A. S. (1993). The rainbow makers: The origins of the synthetic dyestuffs industry in Western Europe. Lehigh University Press.

TS EN ISO 14362-1: (2020). Tekstil — Belirli aromatik aminleri serbest bırakabilen azo boyar maddelerinin tespiti — Bölüm 1: Lifli malzemelerde test için yöntem. Türk Standardları Enstitüsü.

Wang, L., Sun, Y., Yuan, B., & Wang, W. (2018). Occurrence, toxicity and biodegradation of azo dyes in the environment: A review. Ecotoxicology and Environmental Safety, 157, 292–300.

Yılmaz, B., & Gökmen, A. (2020). Azo boyar maddelerin toksikolojik etkileri: Güncel bir değerlendirme. Türk Biyokimya Dergisi, 45(2), 140–150.

Zollinger, H. (2003). Color chemistry: Syntheses, properties, and applications of organic dyes and pigments (3rd ed.). Wiley-VCH.

BÖLÜM 2

SYNTHESIS, CHEMICAL PROPERTIES AND BIOLOGICAL EFFECTS OF THE BENZIMIDAZOLE DERIVATIVES: REVIEW OF LITERATURE

Mehmet PİŞKİN[1]
Mustafa ÖZKAN[2]
Ömer Faruk ÖZTÜRK[3]

INTRODUCTION

The benzimidazole nucleus is an important heterocyclic aromatic organic ring since several of its derivatives have pharmacological properties and have many applications in pharmaceutical chemistry. This compound is bicyclic in nature which consists of the fusion of benzene and imidazole. Many benzimidazole derivatives have different pharmacological properties such as anthelmentic, antiulcer, cardiotonic, antihypertensive. So, they are using antitumor, antifungal, antiparasitic, analgesics, antiviral,

[1] Doç. Dr.,Çanakkale Onsekiz Mart University, Technical Sciences Vocational School, Department of Food Technology, Orcid: 0000-0002-4572-4905
[2] Prof. Dr., Uludağ University, Faculty of Education, Department of Science Education, Orcid: 0000-0002-4380-2279
[3] Prof. Dr., Çanakkale Onsekiz Mart University, Faculty of Science, Department of Chemistry, Orcid: 0000-0002-9244-6805

antihistamine, as well as use in cardiovascular disease, neurology, endocrinology and ophthalmology. Heterocyclic compounds possess a cyclic structure with two or more different kinds of atoms in the ring. These type of compounds are very widely distributed in nature. They are essential to life which are playing a vital role in the metabolism of all living cells e.g. the essential amino acids, proline, histidine, DNA, the vitamins and coenzymes etc. There are a vast number of pharmacologically active heterocyclic compounds, many of which are in regular clinical use. The heterocyclic compounds are used as a synthetic and naturally in medicines and also in pesticides, agrochemicals, polymers etc. The last decades have seen growing interest in the preparation of novel heterocyclic molecules from useful biological activities as well as many other areas. The benzimidazole is important of the wide variety of heterocyclic systems known till date which is in nitrogen heterocyclic species. (Sheehan & ark., 1999; Rida & ark., 2003; Benkli & ark., 2004; Burli & ark., 2005; Hashimoto & ark., 2005; Kazimerczuk, Andrzejewska & Klimesova, 2005; Khalafi & ark., 2005; Mariana & Mercedes, 2005; Sukalovic & ark., 2005; Bhatt & ark., 2023). The benzimidazole nucleus is an important heterocyclic ring since several of its derivatives have pharmacological properties and have been marketed as commercial products. Most significantly, the benzimidazole ring system has been found to be an integral part of Vitamin-B12. Many benzimidazole derivatives have already been reported which different pharmacological properties such as anthelmentic (Habib & ark., 1997), antiulcer (Howden, 1991; McTavish & ark., 1991; Massoomi, Savage & Destache, 1993), cardiotonic (Porai, 1947), antihypertensive (Li & Widdop, 1995). The literature precedence revealed that the substitutions at 1, 2 and 5 positions of the benzimidazole moiety is crucial for the compounds to exhibit wide range of pharmacological activities.

Synthesis of Benzimidazole Derivatives

Detailed reviews covering the synthesis and chemistry of benzimidazole and its derivates have been published. Generally,

benzimidazole derivates can be synthesized from a variety of starting materials and a few of them are listed below in detail.

Acylated o-Nitroarylamine derivatives (Hoebrecker Method)

The first synthesis of benzimidazole, one of the most investigated scaffolds by synthetic chemists, was carried out by Hoebrecker in 1872 by the reduction of 2-nitro-4-methyl acetanilide to synthesize 2,5 (or 2,6) dimethyl benzimidazole derivative, Figure 1 (Hobrecker, 1872; Wright, 1951).

Figure 1

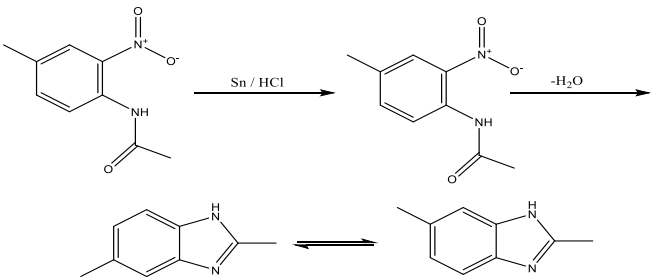

The 2,4,5,6,7-pentamethyl benzimidazole was synthesized as a result of the treatment of 1,2-dinitro-3,4,5,6-tetramethyl benzene with acetic acid under the same reducing conditions, Figure 2 (Smith & Harris, 1935; Smith & Moyle, 1936).

Figure 2

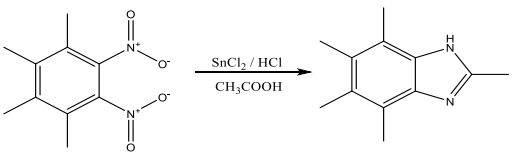

Phillips Method

The heating of o-phenylenediamine and carboxylic acids with dilute HCl resulted in the synthesis of 2-substituted benzimidazole derivatives, Figure 3 (Phillips, 1942).

Figure 3

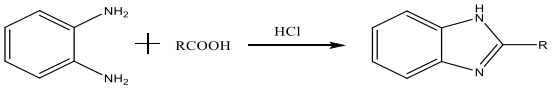

2-Alkyl benzimidazoles were also synthesized by o-phenylenediamine and carboxylated acids. The bis-benzimidazoles were synthesized by heating the *o*-phenylenediamine and dicarboxylic acid in dilute HCl medium, Figure 4 (Pool, Harwood & Ralston, 1937).

Figure 4

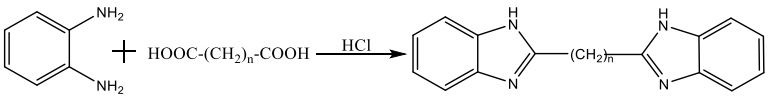

With the reaction of the phenylenediamine with carboxylic acids, 2-alkyl or aryl benzimidazole derivative compounds were synthesized in high yield in the presence of polyphosphoric acid, Figure 5 (Hein, 1957).

Figure 5

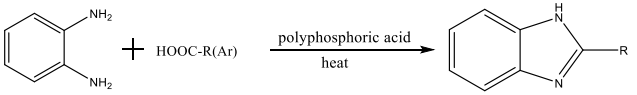

2-substituted benzimidazole derivatives were obtained by ring closure reaction by the treatment of 1,2-diaminobenzene with anthranyl or p-amino benzoic acid in the presence of polyphosphoric acid, Figure 6 (Chhonker & ark., 2009).

Figure 6

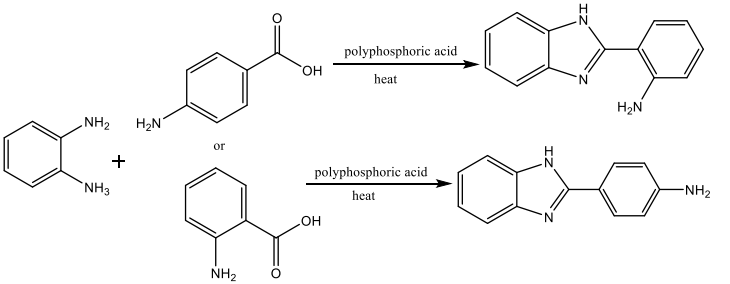

Benzimidazoles from different reactants were synthesized from the reaction of *o*- phenylene- diamine and its derivatives with esters, orthoesters, anhydrides, acid chlorides, nitriles, amides, thioamides and imidates (iminoethers), Figure 7 (Grimmet, 1997).

Figure 7

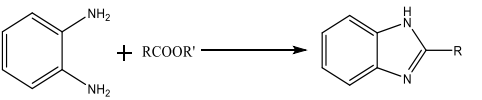

1,2-Diaminobenzene and carboxamides are 2-substituted-1H-benzimidazoles by reaction of ring closure and bisbenzimidazoles by using dicarboxylic diamides, Figure 8 (Townsend & Wise, 1990a).

Figure 8

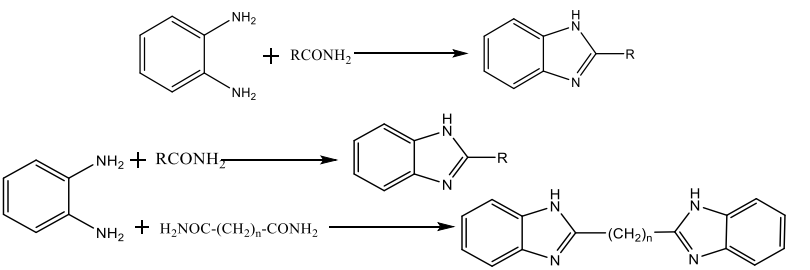

Also; thiabendazole and parbendazole having antihelmintic properties were obtained by the above mentioned method, Figure 9 (Townsend & Wise, 1990b).

Figure 9

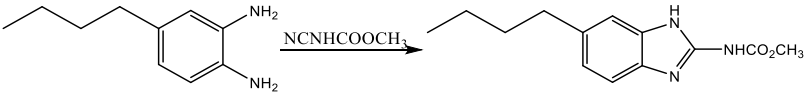

Benzimidazole derivatives were obtained from the ring closure reaction of 1,2-diamino benzene with anhydrides, Figure 10 (Preston, 1974).

Figure10

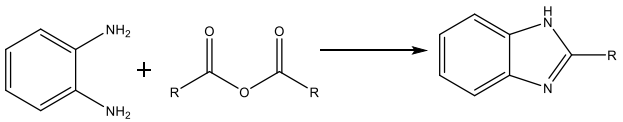

The ring closure reaction of the acid chlorides with o-phenylenediamine derivatives can be synthesized by the benzimidazole derivatives, Figure 11 (Kumar & Joshi, 2007).

Figure 11

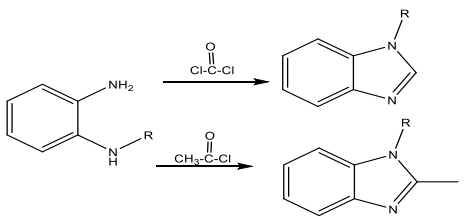

Benzimidazole derivatives were obtained by interaction with nitrites, Figure 12 (Kahveci & ark., 2014).

Figure 12

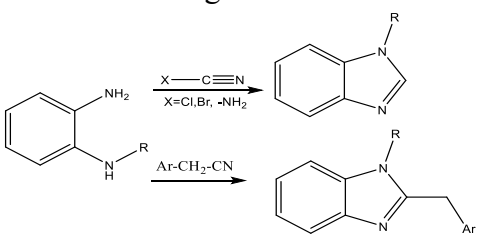

Benzimidazole derivatives were synthesized by ring closure reaction with amides and thioamides, Figure 13 (Kahveci & ark., 2013).

Figure 13

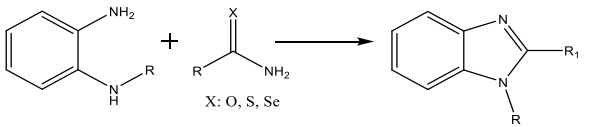

Synthesis of Benzoimidazole Derivative of o-Phenylenediamine and Derivatives with Cyanogen Bromide and Ring Closure

After alkaline treatment of *o*-phenylenediamines with cyanogenbromide in aqueous medium, the 2-aminobenzimidazoles were synthesized as a result of ring closure reaction in a yield ranging from 54-84%, Figure 14 (Lin & ark., 2006a).

Figure 14

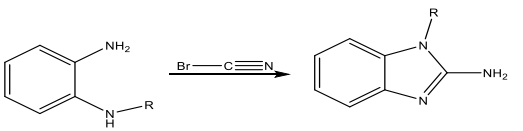

Synthesis of Benzoimidazole Derivatives by Reaction of o-Phenylenediamine and Derivatives with Aldehydes or Ketones

Aldehydes react with o-phenylenediamine and derivatives under oxidizing conditions. In the presence of cerium ammonium nitrate, 1,2-diaminobenzene was treated with various aldehydes to synthesize benzimidazole derivatives, Figure 15 (Lin & ark., 2006b).

Figure 15

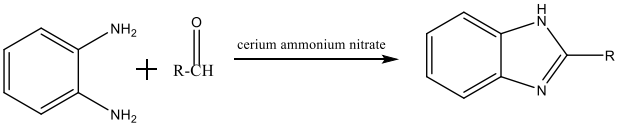

The reaction of o-phenylenediamine and aldehydes in sodium bisulfite salts in N, N-Dimethylformamide was synthesized by 2-arylbenzimidazole derivative compounds, Figure 16 (Pathak & ark., 2010).

Figure 16

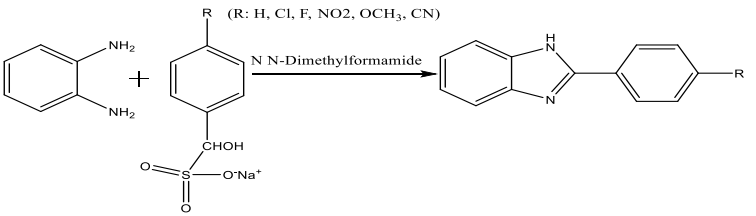

It has been found that it gives good results for the synthesis of the compounds containing the heterocycle group at the aldehyde 2 position (Saleh & ark., 2010). Ketones give the corresponding benzimidazole and hydrocarbon by a similar reaction, Figure 17 (Merck, 1996).

Figure 17

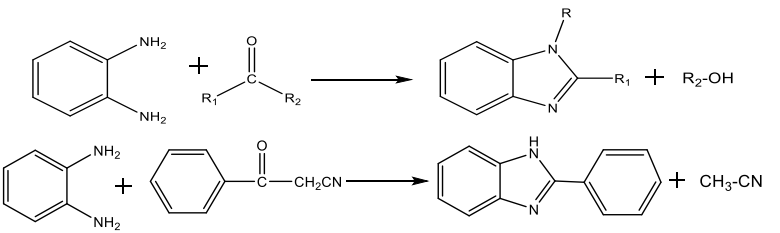

Synthesis of Benzimidazole Derivatives by Microwave Method

Derivatives of o-phenylenediamines were synthesized by microwave method (Osborne, 1969; Rogers & Clayton, 1972).

Benzimidazole reactions were carried out under solution-free conditions with alternative microwave method for the rapid synthesis of pharmacologically important benzimidazoles using an environmentally friendly catalytic amount of $VO(acac)_2$ as catalysts including metal acetylacetonates and organic reactions, Figure 18 (El Kihel &ark., 1999; Chandrakala & ark., 2010).

Figure 18

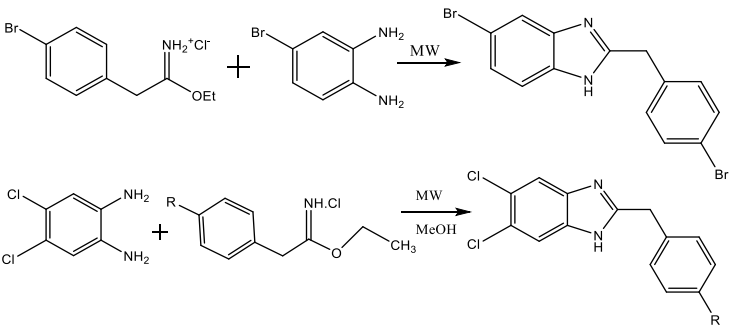

Chemical Properties of Benzimidazole

The benzimidazole ring has a highly stable structure. For example, 1H-benzimidazole is not affected by treatment with HCl or alkalis when heated to 270 °C with sulfuric acid under pressure. Benzimidazole structure of benzene ring can only be oxidized under severe conditions, Figure 19.

Figure 19

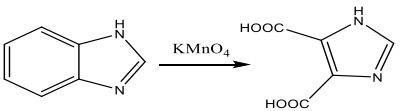

The imidazole ring in benzimidazole is also very resistant to reduction. Even the benzene ring has some resistance to reduction. While benzimidazoles are not reduced by Ni and hydrogen, 2-methyl-2-ethyl and 1,2-dimethylbenzimidazole are converted to their corresponding tetrahydro derivatives when hydrogenated on

platinum oxide in glacial acetic acid. 2-phenylbenzimidazole gives 2-cyclohexyl-4,5,6,7-tetrahydro benzimidazole under these conditions. The chemical activity of the benzimidazole consists of the salt formation of the nitrogens, acylation and alkylation reactions, and the electrophilic substitution reaction of the benzene ring.

Alkylation at the 1-position is fairly rapid when methyl sulfate and alkyl iodide are used. The excess of alkylating reagents is the formation of quaternary salts of benzimidazole. The 1-substituted benzimidazoles often have a low melting point due to insufficient formation of the supported molecules. N-formyl-N,N-dibenzoyl-1,2-diaminobenzene is formed by reacting benzimidazole with benzoyl chloride in the presence of Na_2CO_3. The resulting compound is reacted with NaOH to give the 1,2-dibenzoylaminobenzene compound.

By substitution in benzene ring; nitriding of benzimidazole with concentrated nitric and sulfuric acids produces 5(6)-nitrobenzimidazole, which is a benzimidazole derivative. The position of the nitro group was determined by obtaining the same nitrobenzimidazole from formic acid and 4-nitro-o-phenylenediamine, Figure 20 (Chandrakala & ark., 2010).

Figure 20

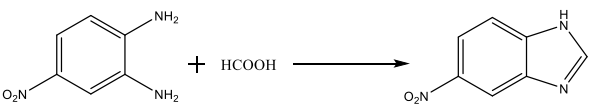

The 2-methylbenzimidazole is reacted with bromine in glacial acetic acid to form 4(7)-brom-2-methylbenzimidazole, Figure 21 (Alamgir, Black & Kumar, 2007).

Figure 21

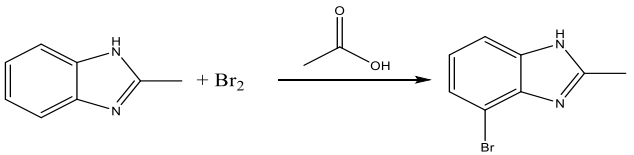

Biological Effects and Uses of Benzimidazole and Derivatives

The new antimicrobial compounds, one of the striking structures is the benzimidazole ring-bearing compounds. Benzimidazole derivative compounds are used as the active ingredient of the drug due to its many effects such as antiulcerative, antihelmintic, antihistaminic, anti-inflammatory and antioxidant (Velik, 2004). Benzimidazole rings may also be purine antimetabolite since they are isosters of the basic structures of DNA bases. Therefore, it is thought that benzimidazole derivative compounds can interact more easily with biopolymers in living systems. In addition, vitamin B_{12} (cyanocobalamin) in the structure of the benzimidazole ring is recognized by living organisms. Again in the literature, astemizole, mebendazole, enviroxime, carbendazim and benzimidazole derivative compounds such as benomyl also inhibit bacterial growth (Zomorodi & Houston, 1995; Atabay, Dulger & Gucin, 2003). Benzimidazole derivative compounds from positions 1, 2, 4, 5 and 6 are known to have a wide range of biological activity (Lance & ark., 1994). Examples of substituted benzimidazole derivative compounds, particularly from 2,4 and 5 (6) positions, are telmisartan, which is currently used as a drug for its antihypertensive activity. Benzimidazole and its derivatives have been extensively studied by transition metal ions. Because such complexes are antitumor, antineoplastic, fungicidal, they show insecticidal, antiviral, antimalarial and other pharmaceutical activities. In these studies, the complexes of Schiff base metal complexes synthesized with dioxygen bonds have recently attracted attention recently. Donor-acceptor effects of amino grams both

catalysts, as well as photochromatic effects and benzimidazole in the biological systems because of the importance has increased. N-heterocyclic compounds especially mono, di and mononuclear or polynuclear structures formed by transition metal complexes with polydentate ligand properties (Loewe & Urbanietz, 1974). Antidepressive, analgesic, antihistaminic, tranculantan, antifungal, neuroleptic, antimicrobial, anticancer, antiarrhythmic and many other effects of these compounds have been found in the studies. Some researchers have determined that the benzimidazole compounds have antihypoxic effect and the body increases the rate of oxygen in case of acute oxygen deficiency (Roderick, 1972). These compounds with benzimidaol derivatives were classified by the World Health Organization as an ATC group (Garcia & Heras, 1981; Popova, 2004). 1,2-bis(2-benzimidazyl)-1,2-ethanediol is a bisbenzimidazole derivative which has shown antiviral character against the antifungal and palio virus (Göker & Terbizli, 1996). Thiabendazole, a thiazole ring substituted benzimidazole derivative from the 2-position, was synthesized and started to be used in the treatment of anthelmintic. Later, the use of Albendazol, Fenbendazole, Mebendazol, Oksfenbendazole, Ttriclabendazole compounds became widespread. Benzimidazoles, which are the active ingredient of the drug, are generally derivatives containing substituents at the 2-, 5-, 6- positions. For antiviral purposes, 2-(α-hydroxybenzyl) benzimidazoles and bisbenzimidazoles have been found to be effective (Göker & ark., 1998). A series of synthesized benzimidazole derivative compounds showed antitumor activity, and these compounds were found to show remarkable efficacy in phase I as an anti-cancer active agent in the treatment of breast cancer (Göker & ark., 2001; Bürli & ark., 2004). These compounds, known as pibenzimol, are fluorescent dyes used to mark DNA in Hoechst dyes fluorescence microscopy and flow cytometry. These dyes are used to stain mitochondria as they mark DNA. Bisbenzimidazole derivative compounds have

been reported to act against rhinovirus, which causes flu and cold (Göker & ark., 2001). Benzimidazole derivatives are also used in commercial drugs as psychopharmacological agents. 5-fluoro-2-(5'-nitro-2'-furyl) benzimidazole and antimicrobial and antifungal activities of the corresponding benzoxazole compounds; The benzimidazole derivative was found to be superior and as a result, the -NH- group in the imidazole ring was found to play an important role in biological activity for these class compounds. Like all nitrogenous heterocycle compounds due to the electron density on nitrogen, benzimidazoles are corrosion inhibitors with strong adsorption properties (Bürli & ark., 2004). As a result of the studies carried out on benzimidazolecarboxamide derivatives, antimicrobial effective derivatives have been reached. It has been reported that derivatives carrying benzimidazole and pyrrole ring systems via carboxamide bridges have a significant antibacterial effect against gram-positive bacteria (Osborne, 1969).

REFERENCES

Alamgir, M., Black, D. C., Kumar, N. (2007). Synthesis, Reactivity and biological activity of benzimidazoles. *Topics of Heterocyclic Chemistry,* 9, 87-118.

Atabay, N. M., Dulger, B., Gucin, F. (2003). Synthesis and İnvestigation of Antimicrobial Activity of Some Bisbenzimidazole-Derived Chelating Agents. *European Journal of Medicinal Chemistry,* 38, 875.

Benkli K., Demirayak S., Gundogdu K. N., Kiraz N., Iscan G., Ucucu U. (2004). *Indian J. Chem.,* 43B, 174.

Bhatt A. K., Karadiya H., Shah P. R., Parmar M. P., Patel H. D. (2003). *Indian J. Het. Chem.,* 13, 187.

Burli R. W., McMinn Dustin, Kaizerman J. A., Hu W., Ge Y., Pack Q., Jiang, V., Gross M., Garcia M., Tanaka R., Moser H. E. (2005). *Bioorg & Med. Chem. Lett.,* 14, 1253.

Bürli, R. W., Mcminn, D., Kaizerman, J. A., Hu, W., Ge, Y., Pack, Q., Jiang, V., Gross, M., Garcia, M., Tanaka, R., Moser, H. E. (2004). DNA binding ligands targeting drug-resistant Gram-positive bacteria. Part 1: Internal benzimidazole derivatives, *Bioorganic Medicinal Chemistry Letters,* 14, 1253.

Chandrakala, M., Sheshadri, B. S., Gowda, N. M. N., Murthy, K. G. S. ve Nagasundara, K. R. (2010). Synthesis and spectral studies of 2-salicylidine-4-aminophenylbenzimidazole and its reaction with divalent Zn, Cd and Hg: crystal structure of the cadmium bromide complex, *Journal of Chemical Research,* 10, 576.

Chhonker Y. S., Veenu B., Hasim S. R. and Kumar D. (2009). Synthesis and Pharmacological Evaluation of Some New 2-phenyl Benzimidazoles Derivatives and Their Schiff's Bases. *E-Journal of Chemistry,* 6, 342.

El Kihel, A., Benchidmi, M., Essassi, E. M., Danion-Bougot, R. (1999). Halogenation of Substituted Benzimidazoles. Nitration of the Resulting Halobenzimidazoles, *Synthetic Comminication,* 29, 387.

Garcia, M.T., Heras, F. G. D. (1981). *Medicinal Chemistry Advences*, Pergamon Press, 5. Edition, 69.

Göker, H., Terbizli, E. (1996). Synthesis of 1,2-Disubstituted Benzimidazole-5(6)- Carboxamides and Evaluation of Their Antimicrobial Activity. *Farmaco,* 51(1), 53.

Göker, H., Tunçbilek, M., Ayhan, G., Altanlar, N. (1998). Synthesis of some new benzimidazolecarboxamides and evaluation of their antimicrobial activity. *Farmaco,* 55(2), 12.

Göker, H., Tunçbilek, M., Süzen, S., Kuş, C., Altanlar, N. (2001). Synthesis and Antimicrobial Activity of Some New N-Substituted carboxyamido-1H-benzimidazole Derivatives, *Pharmaceutical & Medicinal Chemistry,* 334, 148.

Grimmet, M. R. (1997). *Best Synthetic Methods-Key Systems and Functional Groups, Imidazole and Benzimidazole Synthesis.* Series Editor, Menth-Cohn O. Academic Pres, Inc, San Diego, Calfornia, 19-88.

Habib N. S., Soliman R., Ashour F. A., El-Taiebi M. (1997). *Pharmazie*, 52, 74.

Hashimoto K., Tatsuta M., Yasoshima K., Shogase Y., Shimazaki M., Yura T., Li Y., Urbahns K., Yamamoto N., Gupta J. B. (2005). *Bioorg. & Med. Chem. Lett.,* 15, 799.

Hein, D. W. (1957). The use of Polyphosporic Acid in the Synthesis of 2-Aryl- and 2-Alkyl-substituted Benzimidazoles, Benzoxazoles and Benzothiozoles, *J. American Chemical Society,* 79, 427.

Hobrecker, F. (1872). *Ber. Dtsch. Chem. Ges.,* 5, 290.

Howden, C. W. (1991). Clin. Pharmacokinetics, 20, 38. *J. Wright, Chem. Rev.,* (1951) 48, 397.

Kahveci B., Menteşe E., Özil M., Ülker S., Ertürk M. (2013). An efficient synthesis of benzimidazoles via a microwave technique and evaluation of their biological activities. *Monatsh Chemistry,* 144, 993.

Kahveci B., Yılmaz F., Menteşe E., Özil M., Karoğlu, A. (2014). Microwave-Assisted Synthesis of Some Novel Benzimidazole Derivatives Containing Imine Function and Evaluation of Their Antimicrobial Activity. *Journal of Heterocyclic Chemistry,* 51, 982.

Kazimerczuk Z., Andrzejewska M., Klimesova V. (2005). *Eur. J. Med Chem.,* 40, 203.

Khalafi N. A., Soltani Rad M. N., Mohabatkar H., Ansari Z., Hemmateenejad B. (2005). *Bioorg. & Med. Chem.,* 13, 1931.

Kumar, R., Joshi, Y. C. (2007). Mild and Efficient One Pot Synthesis of Imidazolines and Benzimidazoles from Aldehydes. *E-Journal of Chemistry,* 4, 606.

Lance Gravatt, G., Baguley, B. C., Wilson, R. W., Baguley, W. C., Wilson, W. R., Denny, W. A. (1994). DNA-Directed Alkylating Agents. Syenthesis and Antitumor Activity of DNA minor Groove-Targeted Aniline Mustard Analogues of Pibenzimol (Hoechts33258). *Journal of Medicinal Chemistry,* 37, 433.

Li X. C., Widdop R. E. (1995). *Hypertension,* 26, 989.

Lin, S. Y., Isome, Y., Stewart, E., Liu, J. F., Yohannes, D., Yu, L. B. (2006a). Microwave-assisted one step high-throughput synthesis of benzimidazoles, *Tetrahedron Letters,* 47 (17), 2883.

Lin, S. Y., Isome, Y., Yohannes, D., Yu, L. B. ve Liu, J. F. (2006b) Microwave-assisted one-step synthesis of benzimidazoles, *American Chemical Society,* 231.

Loewe, H. J., Urbanietz. (1974). Basisch Substituerte 2,6-Bisbenzimidazolderivatives, Eine Neue Chemotherapeutisch Active Korper Classe (2,6-Bisbenzimidazoles with Basic Substituents a New Class of Chemotherapeutically Active Compounds). *Arzneim-Forsch,* 24, 1927.

Mariana B. (2005). Mercedes G., Mini-Reviews in Med. *Chem.,* 5, 409.

Massoomi F., Savage J., Destache C. J. (1993). *Pharmacotherapy,* 13, 46.

McTavish D., Buckley M. M. T., Heel R. T. (1991). *Drugs,* 42, 138.

Merck, Co. (1996). *The Merck Index, An Encyclopedia of Chemical Drugs and Biologicals*, 12th . Ed., Whitehouse Station NJ, USA.

Osborne DRD. (Unilever Ltd.). (1969). *Antibacterial Anilinobenzimidazoles*. Brit. Patent 1,171,904, Ref. Heterocyclic Compounds, 72: 31797-1970.

Pathak D., Siddiqui N., Bhrigu B., Ahsan W. (2010). Alam MS. Benzimidazoles: A New Profile of Biological Activities. *Der Pharmacia Lettre,*2(2): 27.

Phillips, M. A. (1942). Bis–Benzimidazoles. *J. American Chemical Society*, 64, 187.

Pool, W. O., Harwood, H. J., Ralston, A. W. (1937). 2-Alkylbenzimidazoles as Derivatives for the Identification of Aliphatic Acids, *J. American Chemical Society,* 59, 178.

Popova, A., Christov, M., Raicheva, S., Sokolova, E. (2004). Adsorption and inhibitive properties of benzimidazole derivatives in acid mild steel corrosion. *Corrosion Science,* 46, 1333.

Porai Koshits B. A., Ginzburg S. F., Etros L. S. (1947). *Zh. Obshch. Khim., 768*; *Chem. Abstr.,* (1948) 42, 5903.

Preston, P. N. (1974). Synthesis Reactions and Spectroscopic Properties of Benzimidazoles, *Chemical Rewiews,* 74, 279.

Rida S. M., Shafik R. M., Ashour F. A., Youssef A. M. (2003). *J. Pharmaceutical Sciences.,* 17, 125.

Roderick, W. R., Nordeen, C. W., Von Esch, A. M., Appell, R. N. (1972). Bisbenzimidalozes: Potent Inhibitors of Rhinoviruses. *Journal of Medicinal Chemistry,* 15, 655.

Rogers, K. S., and Clayton, C. C. (1972). The Effects of Ph on benzimidazole Fluorescence. *Analytical Biochemistry,* 48, 199.

Saleh M, Abbott S, Lauzon VC, Penney C, Zacharie B. (2010) Synthesis and antimicrobial activity of 2-fluorophenyl-4,6-disubstituted [1,3,5]triazines. *Bioorg Med Chem Lett.,* 20, 945.

Sheehan D. J., Hitchcock C. A., Sibley C. M. (1999). *Clinical Microbiol. Rev.,* 12, 40.

Smith, L. I., Harris, S. A. (1935). Studies on the Polymethylbenzenes. The Nitration of Pentamrthylbenzene and of Hexamethyl and Hexaethylbenzene, *J. American Chemical Society,* 57, 1289.

Smith, L. I., Moyle, C. L. (1936). The Jacobsen Reaction, *J. American Chemical Society,* 58, 1.

Sukalovic V., Andric D., Roglic G., Sladjana K. R., Schratteholz A., Soskis V. (2005). E*ur. J. Med. Chem.,* 40, 481.

Townsend, L. B., Wise, D. S. (1990). The Synthesis and Chemistry of Certain Anthelmintic Benzimidazoles. *Parasitology Today,* 6, 107.

Velik, J., Baliharova, V., Frink-Gremmels, J., Bull, S., Lamka, J., Skalova, L. (2004). Benzimidazole drugs and modulation of biotransformation enzymes. *Research in Veterinary Science,* 76, 95.

Zomorodi, K., Houston, J. B. (1995). Effect of omeprazole on diazepam disposition in rat: In vitro and in vivo studies. *Pharmacological Research,* 12, 1642.

BÖLÜM 3

SYNTHESIS AND APPLICATION OF TITANIUM-BASED METAL-ORGANIC FRAMEWORK IN PHOTOCATALYTIC DEGRADATION OF SOME ORGANIC DYES

PELİN SÖZEN AKTAŞ[1]
KADER ÖKTEM[2]

INTRODUCTION

Metal organic frameworks (MOFs) are materials that have experienced significant development during the last thirty years since their introduction by Yaghi and co-workers in 1995 (Yaghi et al., 1995). This progress is due to their large surface area, customizable pore sizes, and varied functionality groups. MOF materials present considerable potential for many applications, including catalysis (J. Li et al., 2023), pollutant removal (Drout et al., 2019; Su et al., 2025), medication delivery, biomedical field (Sun et al., 2020), gas storage, adsorption, and separation (Vellingiri et al., 2017).

[1] Assoc.Prof. Dr, Manisa Celal Bayar University, Department of Chemistry, Orcid: 0000-0003-2140-2650
[2] Manisa Celal Bayar University, The Graduate School, Orcıd:0009-0006-5451-2222

MOFs have gained attention in photocatalysis due to their high surface area, adjustable structure, and dense active sites. They have been extensively investigated in the removal of organic pollutants caused by their structural and fascinating features (J. Li et al., 2023; Yao et al., 2018). Industrial activities in textiles, paper, and leather have generated significant amounts of wastewater containing various organic dyes, which often lead to serious environmental issues and might threaten human health (L. Li et al., 2020). Photodegradation of organic dyes presents a promising solution to this environmental issue. Among the various photocatalysts used for this purpose, highly porous metal-organic frameworks (MOFs) exhibit diverse structures and offer adjustable functionalities, such as the elimination of organic dyes through photodegradation. In contrast to other MOFs, Ti-based MOFs have potential applications in this subject and area. Gao and co-workers reported NTU-9, Ti-MOF, which demonstrated p-type semiconductor behavior and displayed excellent photocatalytic activity in degrading MB and rhodamine B dyes (Gao et al., 2014). A porphyrinic Ti-MOF and NH_2-MIL-125 were employed as catalysts to degrade Rh B under various light sources. In the visible region, the photocatalytic degradation efficacy of porphyrinic Ti-MOF outperforms that of NH_2-MIL-125 MOFs. (X. Guo et al., 2021). In another study, MIL-125 and NH_2-MIL-125 were prepared using the solvothermal method and showed effective degradation of MB when exposed to visible light (Mahmoodi et al., 2024). Studies on removing organic pollutants by Ti-MOFs containing terephthalic acid and amino groups are ongoing. The MIP-207 structure, which contains trimesic acid, is stable in water and has high porosity, making it a good candidate for catalysis studies. Serre and colleagues used pre-prepared titanium-oxygen clusters to self-assemble trimesic acid, resulting in the controlled synthesis of MIP-207, which remained stable in water for over three days (Wang et al., 2020).

In this study, the MIP-207 Ti-MOF structure was synthesized using the method described in the literature and utilized as a catalyst to remove dyes (MB and MO) from an aqueous solution. Furthermore, the structures of the prepared MIP-207 were characterized by XRD, TGA, FT-IR, and BET surface area analysis before catalytic activity was assessed. M1 and M2 were evaluated as photocatalysts for decolorizing methylene blue (MB) and methyl orange (MO)exposed to UV light irradiation; the M1 structure demonstrated higher photocatalytic activity for both dyes. It was found that the M1 structure synthesized using the solvothermal method exhibited more significant activity in removing both MB and MO under UV light, attributed to its surface area and more uniform structure.

METHOD

All reagents used were of analytical grade and were employed without any further modification or purification. Titanium(IV) isopropoxide (97%, Sigma-Aldrich), trimesic acid (95%, Sigma Aldrich), acetic acid (glacial, Merck), acetic anhydride (96%, Merck), DMF (99.8%, Merck), acetone (Isolab), methanol (Isolab), and MB(methylene blue) (BDH), and MO(methyl orange) (Carlo Erba) were used as received. MIP-207 was synthesized with a minor modification following the methodology described in the literature (Wang et al., 2020).

Synthesis of Ti-based MOF, MIP-207 (M1) in the Teflon-coated PTFE inner chamber (Method 1)

Ti(IV) isopropoxide (0.306 mL, 1 mmol) was added to trimesic acid (0.328 g, 1.5 mmol) in 2.5 mL of acetic acid and 2.5 mL of acetic anhydride solution. The solution, transferred to the Teflon-coated PTFE inner chamber cell, was heated in a vacuum oven at 120 °C for 48 hours in the reactor system and then cooled to r.t. The white precipitate was filtered out from the solution and rinsed with

acetone. The obtained powder (0.4823 g) was dried at 100 °C in a vacuum oven. The diagrammatic illustration of the synthesis is given in Figure 1.

Synthesis of Ti-based MOF, MIP-207(M2) by reflux (Method 2)

Ti(IV) isopropoxide (1 mL, 3.27 mmol) was added to a solution of trimesic acid (1.05 g, 4.75 mmol) in 12.5 mL of acetic acid and 12.5 mL of acetic anhydride in a 100 mL Schlenk flask and refluxed at 120 °C for 24 hours. The mixture was then cooled to r.t. The white precipitate was filtered from the solution and then rinsed with acetone. The resulting powder (1.2567 g) was dried at 100 °C in a vacuum oven.

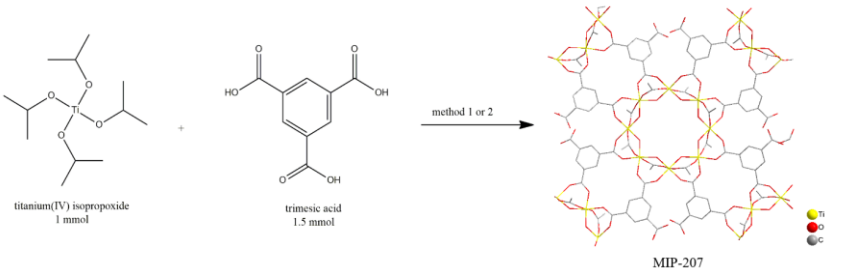

Figure 1. *Synthesis route for MIP-207*

Characterization and Photocatalytic Activity

XRD patterns of the MIP-207 powders were measured by a PANalytical Empyrean diffractometer with Cu Kα (λ= 1.5406Å) X-ray radiation (40 mA, 45 kV). The FT-IR spectra of the samples were measured at r.t. by a Perkin Elmer FT-IR system (Spectrum BX). Thermogravimetric analysis was performed on a TA Instruments SDT 650 simultaneous thermal analyzer. The Match! Version 3 Crystal Impact program was used for phase-identification (Putz & Brandenburg). The XRD patterns of the obtained compounds were analyzed with the Rietveld refinement program FULLPROF (Rodríguez-Carvajal, 1993). BET measurements were performed

with a Micromeritics Gemini VII 2390t instrument. The MIP-207 powders were also characterized by an SEM equipped with an EDS (Zeiss Gemini 500). We tested photocatalytic activity using an experimental setup featuring an OUSIDE E27 lamp at a power of 15 W (395-400 nm UV-A). We utilized a Perkin Elmer UV-VIS Lambda 365 spectrophotometer to measure the UV-Visible absorption spectrum of the samples.

RESULTS and DISCUSSION

Characterization of Ti-MOF structures

The synthesized Ti-MOFs were characterized with several methods as indicated below. XRD was conducted to examine the crystal structure of M1 and M2 MIP-207 samples. The XRD patterns for M1 and M2, generated by two distinct methods, are depicted in Figure 2. Figure 3 presents the Rietveld refinement of M1 and M2, demonstrating consistency with the data reported by Wang and colleagues (Wang et al., 2020). XRD patterns of M1 and M2 show peaks at 5.16 °, 10.30 °, 11.40°, 15.44°, 16.22°, 18.64°, 21.42°, 23.23° values. All findings are consistent with the reported results data. This referenced data pattern was utilized for the Rietveld refinement implemented in Match! Software. The results suggest that M1 and M2 are in the tetragonal space group P 4/n b m (#125). Refinement, lattice, and structural parameters are given in Table 1. The refined structure of M1 is given in Figure 2 (b). The results indicated that the Rietveld analysis and the XRD of the prepared MIP-207 correlated with those documented in the literature data (Wang et al., 2020).

Figure 2. *XRD patterns of MIP-207 powders with different methods (a), Refined structure of M1(b)*

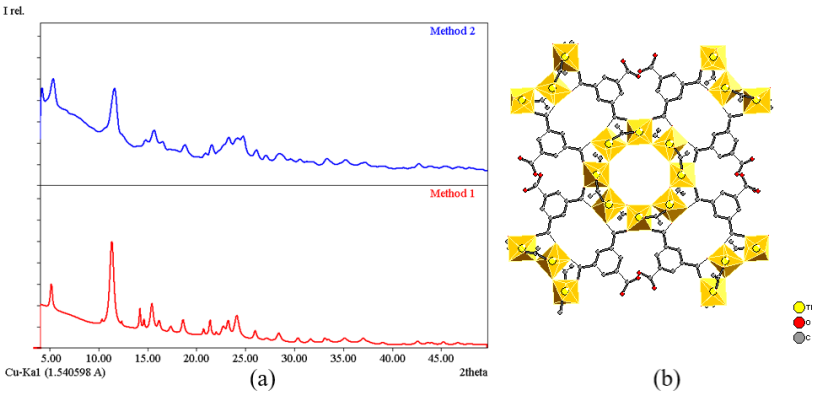

Table 1. *Rietveld refinement, lattice and crystallite size, surface characteristic parameters for MIP-207 samples*

MIP-207 sample	M1	M2
Formula		
T, λ, data range, step size	298 K, 1.54060Å, 4.036°-50.015°,0.013	
Space group, crystal system	Tetragonal P 4/n b m (#125)	
Unit cell parameters	a=24.1899 (3) Å, c=7.8106 (3) Å, α=90°	a=24.2762 (2) Å, c=7.8606 (3) Å, α=90°
Volume ($Å^3$)	4570.43	4632.58
Density (g/cm^3)	1.421	1.403
R_p, R_{wp}, R_{exp}, χ^2	19.2, 19.6, 8.80, 4.97	49.4, 48.1, 19.29, 6.23
Average crystallite size (nm)	26.01	29.16

Figure 3. *Rietveld refinement of M1 and M2 (1. observed, 2. calculated, 3. difference, 4. Bragg positions)*

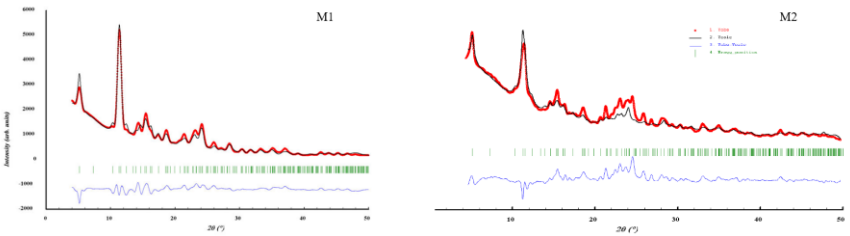

For further characterization, the IR spectra of trimesic acid, M1, and M2 are shown in Figures 4 and 5, respectively. The infrared spectra of trimesic acid and Ti-MOFs exhibit significant differences from one another. Trimesic acid exhibits characteristic C=O and C-O stretching vibrations at 1721 cm^{-1}, and 1405-1327 cm^{-1}. The spectral bands detected at 1276-1107 cm^{1} and 916 cm^{1} are attributed to the in- and out- planes stretching vibrations of the C-H groups of benzene. Additionally, C-C (benzene ring) stretching vibrations are observed at 1455 cm^{-1}. (Mahalakshmi et al., 2014). . The spectra of M1 and M2 contain bands at 1708 cm^{-1} (C=O) and 1448, 1376 cm^{-1} (C-O), that have moved to lower frequencies in comparison to acid. M1 and M2 exhibit a wide band at 3563 cm^{-1}, suggesting the presence of adsorbed water. Using anhydride and carboxylic acid in the synthesis reaction can form structures containing MOFs-(COOH) that can be removed by heating. The peaks observed at 2628 cm^{-1} and 2550 cm^{-1} can be attributed to H- bonded carboxylic acid groups. An analogous situation has been observed for some MOF structures (Hadjiivanov et al., 2021)The FTIR spectrum of the MOFs displays distinct O-Ti-O bands in the range of 400 to 800 cm^{-1}. Peaks observed at 507.5 and 446.9 cm^{-1} correspond to these stretching vibrations (George et al., 2017; H. Guo et al., 2015).

Figure 4. *FTIR spectrum of trimesic acid*

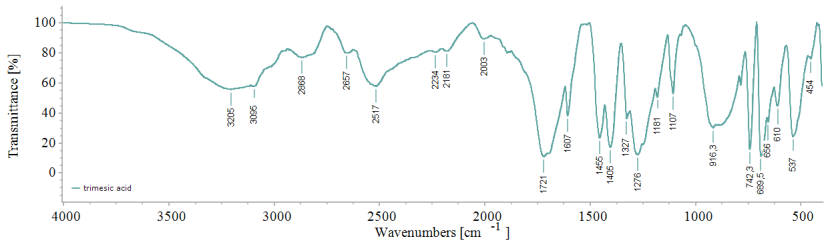

Figure 5. *FTIR spectra of MIP-207 samples*

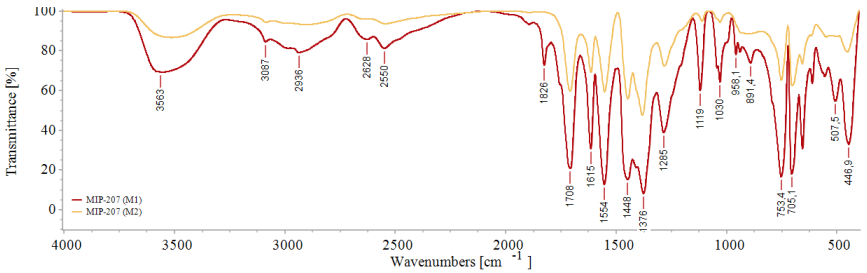

TGA methodology was used for MOFs to understand thermal decomposition steps of components correlated to temperature. Figure 6 shows TGA plots of M1 and M2 between 25 °C and 1000 °C. M1 and M2 consisted of three main steps, where both lost app. 5 % by weight of adsorbed water at 100 °C. Between 200 °C and 300 °C, the weight lost is by app. 15%, corresponding to the removal of solvent molecules adsorbed on the surface of M1 and M2(Lázaro, 2020) . It has been observed that while some fragments are detached at temperatures ranging from 300 °C to 550 °C, the structure maintains stability between 600 °C and 800 °C, and it commences decomposition at temperatures exceeding this range.

The experimentally measured BET surface areas for M1 and M2 were 439.57 m^2/g and 430.45 m^2/g, respectively, both of which are lower than the data that have been reported (Wang et al., 2020). Surface characteristic parameters, total pore volume, and pore size data are also presented in Table 2.

Figure 6. *TGA plots of MIP-207 samples*

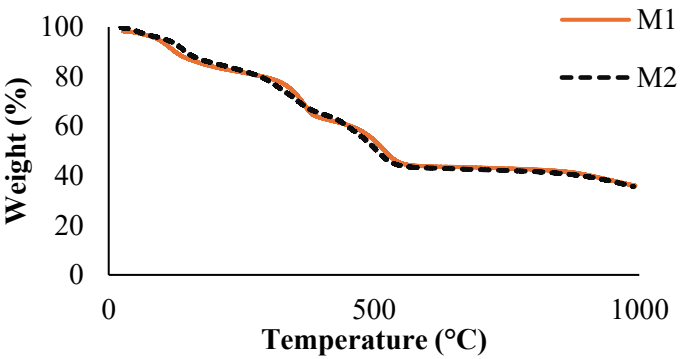

Table 2. *Surface characteristic parameters for MIP-207 samples*

	BET Surface area S_{BET}[m^2g^{-1}]	Total pore volume $V_{T,}$ [cm^3g^{-1}]	Pore size[nm]
M1	439.5746	0.2945	25.48
M2	430.4597	0.1810	9.36

Figure 7 illustrates the morphology of M1 (a, b, c) and M2 (d, e, f) samples. The SEM images of M1, shown in Figure 7 (a-c), display a distribution of neatly arranged flower-like forms featuring multiple layers. In Figure 7 (d-f), the M2 structure appears distributed as irregularly shaped rod clusters. Both structures were observed to contain pores. In the M1 and M2 structures synthesized using two different methods, it was determined that the M1 synthesis route achieved a larger surface area and more uniform material. This influenced the photocatalytic activity of the structure, with M1 demonstrating greater activity.

Figure 7. *SEM images of samples M1 (a: 5.00 KX, b: 10.00 KX, c: 20.00 KX) and M2 (d: 10.00 KX, e: 20.00 KX, f: 50.00 KX magnification)*

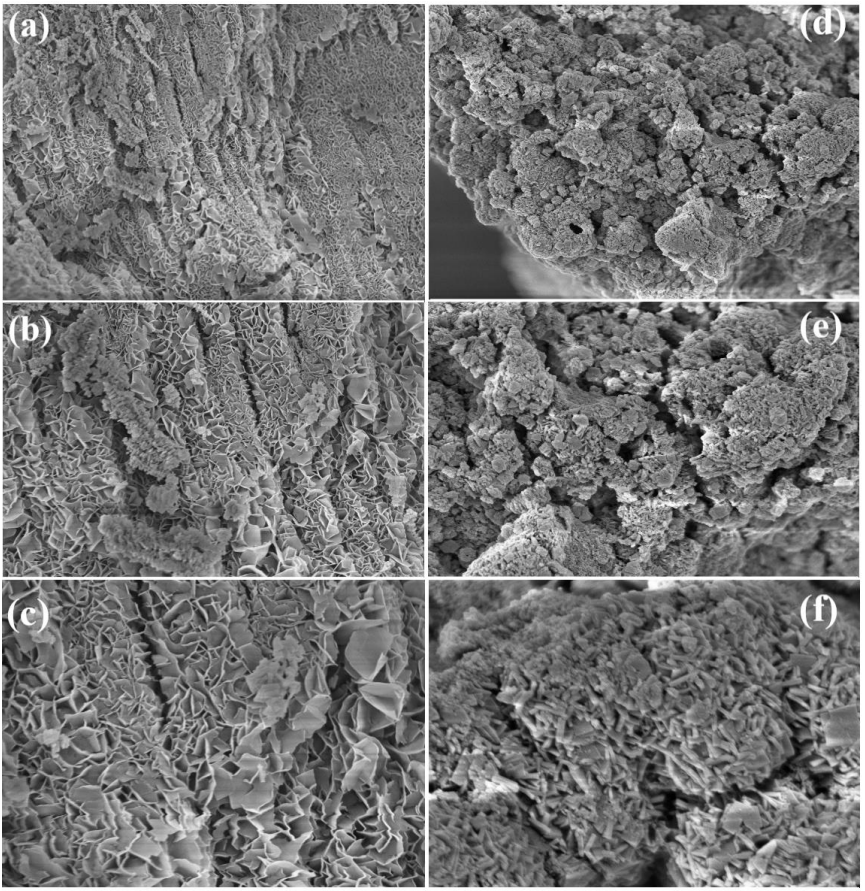

Photocatalytic Degradation of Organic Dyes

We evaluated the photocatalytic activity of the synthesized MIP-207 structures during the photodegradation of MB and MO when exposed to UV light. The degradation reaction of methylene blue with MIP-207 (M1) catalyst was carried out for 330 min. 10 mg of MIP-207 (M1) catalyst was added to 100 mL of 10 ppm methylene blue solution. After stirring for 5 min, it remained in the dark for 30

minutes, for absorption/desorption balance and 3 mL was taken and centrifugated at 30x100 rpm for 1 min and absorbance was measured (0 min.). It was stirred at 300 rpm under UV light for a total of 330 min, and 3 mL was taken in 30-minute periods and centrifuged at 30x100 rpm for 1 min, and the absorbance of the solution was measured. Similar procedures were repeated for methyl orange at the same stoichiometric ratio. The degradation efficiency of dyes is calculated by the formula % $=(C_0\text{-}C)/C_0$ x 100, where C_0 is the starting concentration (mg/L) and C represents the concentration (mg/L) at a specific time. The characteristic maximum absorbance of methylene blue is seen at 663 nm. UV-vis spectra taken at certain time intervals during the photodegradation of methylene blue under M1 and M2 catalysts are given in Figure 8. While approximately 82% of methylene blue was degraded at the end of 330 minutes under M1 catalyst (as seen in Figure 9), it was observed that approximately 40% was decolorized at the end of 120 minutes in the presence of M2.

Figure 8. *UV-VIS spectra of MB over time with M1 and M2 catalyst*

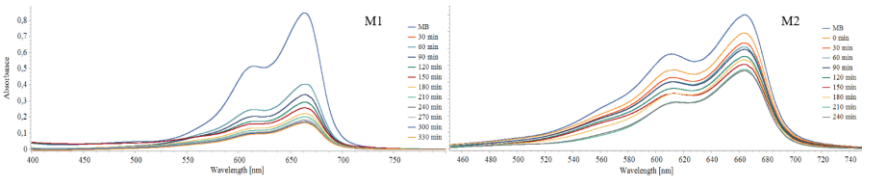

Figure 9. *Photocatalytic activity of M1 and M2 samples*

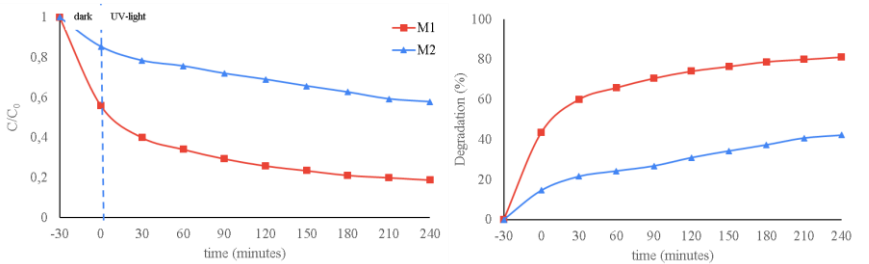

The maximum absorbance of methyl orange occurs at 465 nm. The UV-vis spectra collected at specific time intervals during photodegradation with catalysts M1 and M2 are presented in Figure 10. After 120 minutes, about 40% of methyl orange was degraded with M1, while with M2, the degradation was 22%.

Figure 10. *Time-varying UV-VIS spectra of MO with M1 and M2 catalysts*

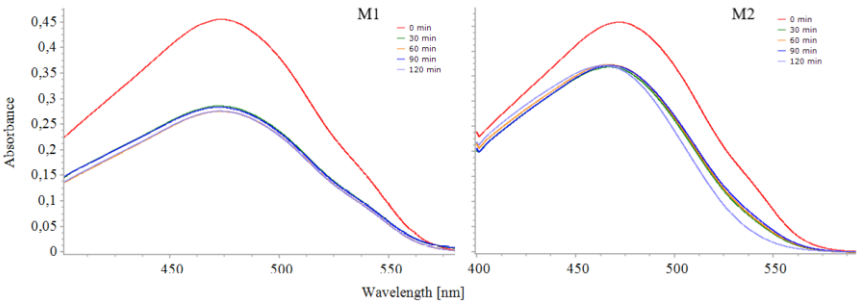

CONCLUSION

In the present work, two methods were used to prepare M1 and M2 photocatalysts. The M1 structure synthesized by the solvothermal method showed higher activity in removing both MB and MO under UV light because of its larger surface area and more uniformity. SEM analysis showed that both structures were porous; the M1 structure was more regular. Similarly, BET results showed that the M1 surface area, total pore volume, and pore size were larger, measured as 439.57 m^2/g, 0.2945 cm^3/g, and 25.48 nm, respectively. The synthesis of the MIP-207 structure by the solvothermal method was also practical on photocatalytic activity. The M2 structure removed 82% of the MB dye in 330 minutes.

REFERENCES

Drout, R. J., Robison, L., Chen, Z., Islamoglu, T., & Farha, O. K. (2019). Zirconium Metal–Organic Frameworks for Organic Pollutant Adsorption. In Trends in Chemistry (Vol. 1, Issue 3, pp. 304–317). Cell Press. doi: 10.1016/j.trechm.2019.03.010

Gao, J., Miao, J., Li, P. Z., Teng, W. Y., Yang, L., Zhao, Y., Liu, B., & Zhang, Q. (2014). A p–type Ti(iv)–based metal–organic framework with visible–light photo–response. Chemical Communications, 50(29), 3786–3788. doi: 10.1039/c3cc49440c

George, P., Dhabarde, N. R., & Chowdhury, P. (2017). Rapid synthesis of Titanium based Metal Organic framework (MIL-125) via microwave route and its performance evaluation in photocatalysis. Materials Letters, 186, 151–154. doi: 10.1016/j.matlet.2016.09.099

Guo, H., Lin, F., Chen, J., Li, F., & Weng, W. (2015). Metal-organic framework MIL-125(Ti) for efficient adsorptive removal of Rhodamine B from aqueous solution. Applied Organometallic Chemistry, 29(1), 12–19. doi: 10.1002/aoc.3237

Guo, X., Tian, X., Xu, X., & He, J. (2021). Enhancing visible-light-activity of Ti-based MOFs based on extending the conjugated degree of organic ligands and photocatalytic degradation process and mechanism in real industrial textile wastewaters. Journal of Environmental Chemical Engineering, 9(6). doi: 10.1016/j.jece.2021.106428

Hadjiivanov, K. I., Panayotov, D. A., Mihaylov, M. Y., Ivanova, E. Z., Chakarova, K. K., Andonova, S. M., & Drenchev, N. L. (2021). Power of Infrared and Raman Spectroscopies to Characterize Metal-Organic Frameworks and Investigate Their Interaction with Guest Molecules. In Chemical Reviews (Vol. 121,

Issue 3, pp. 1286–1424). American Chemical Society. doi: 10.1021/acs.chemrev.0c00487

Lázaro, I. A. (2020). A Comprehensive Thermogravimetric Analysis Multifaceted Method for the Exact Determination of the Composition of Multifunctional Metal-Organic Framework Materials. European Journal of Inorganic Chemistry, 2020(45), 4284–4294. doi: 10.1002/ejic.202000656

Li, J., Huang, J. Y., Meng, Y. X., Li, L., Zhang, L. L., & Jiang, H. L. (2023). Zr- and Ti-based metal-organic frameworks: synthesis, structures and catalytic applications. Chemical Communications, 59(18), 2541–2559. doi: 10.1039/d2cc06948b

Li, L., Wang, X. S., Liu, T. F., & Ye, J. (2020). Titanium-Based MOF Materials: From Crystal Engineering to Photocatalysis. In Small Methods (Vol. 4, Issue 12). John Wiley and Sons Inc. doi: 10.1002/smtd.202000486

Mahalakshmi, G., & Balachandran, V. (2014). FT-IR and FT-Raman spectra, normal coordinate analysis and ab initio computations of Trimesic acid. Spectrochimica Acta - Part A: Molecular and Biomolecular Spectroscopy, 124, 535–547. doi: 10.1016/j.saa.2014.01.061

Mahmoodi, A., Dorranian, D., & Abbasi, H. (2024). Significant effects of negligible amount of H2O2 on photocatalytic efficiency of MIL-125 and NH2-MIL-125 nanostructures in degradation of methylene blue. RSC Advances, 14(41), 30140–30153. doi: 10.1039/d4ra05733c

Putz H, & Brandenburg K. Match! - Phase Identification from Powder Diffraction, Crystal Impact - Dr. H. Putz & Dr. K. Brandenburg GbR, Kreuzherrenstr. 102, 53227 Bonn, Germany, Http://www.crystalimpact.com/match.

Rodríguez-Carvajal, J. (1993). Recent advances in magnetic structure determination by neutron powder diffraction. Physica B: Physics of Condensed Matter, 192(1–2), 55–69. doi: 10.1016/0921-4526(93)90108-I

Su, R., Yao, H., Wang, H., Chen, Y., Huang, S., Luo, Y., & Ma, X. (2025). Metal-organic frameworks for removing emerging organic pollutants: A review. In Journal of Water Process Engineering (Vol. 70). Elsevier Ltd. doi: 10.1016/j.jwpe.2025.107096

Sun, Y., Zheng, L., Yang, Y., Qian, X., Fu, T., Li, X., Yang, Z., Yan, H., Cui, C., & Tan, W. (2020). Metal–Organic Framework Nanocarriers for Drug Delivery in Biomedical Applications. In Nano-Micro Letters (Vol. 12, Issue 1). Springer. doi: 10.1007/s40820-020-00423-3

Vellingiri, K., Kumar, P., Deep, A., & Kim, K. H. (2017). Metal-organic frameworks for the adsorption of gaseous toluene under ambient temperature and pressure. Chemical Engineering Journal, 307, 1116–1126. doi: 10.1016/j.cej.2016.09.012

Wang, S., Reinsch, H., Heymans, N., Wahiduzzaman, M., Martineau-Corcos, C., De Weireld, G., Maurin, G., & Serre, C. (2020). Toward a Rational Design of Titanium Metal-Organic Frameworks. Matter, 2(2), 440–450. doi: 10.1016/j.matt.2019.11.002

Yaghi, . M, & Li, H. (1995). Hydrothermal Synthesis of a Metal-Organic Framework Containing Large Rectangular Channels. In J. Am. Chem. SOC (Vol. 117).

Yao, P., Liu, H., Wang, D., Chen, J., Li, G., & An, T. (2018). Enhanced visible-light photocatalytic activity to volatile organic compounds degradation and deactivation resistance mechanism of titania confined inside a metal-organic framework. Journal of

Colloid and Interface Science, 522, 174–182. doi: 10.1016/j.jcis.2018.03.075.

BÖLÜM 4

NEW HETEROCYCLİC AZO DYE POLYMERS: SYNTHESİS, CHARACTERİZATİON AND THERMAL STABİLİTY STUDİES

DİLEK ÇANAKÇI[1]

INTRODUCTİON

When it comes to dyes, the first thing that comes to mind is substances with very high light absorption. For this reason, a very small amount of dye is sufficient for a unit of fabric to dye fabrics or to make print dyes. Before the production of synthetic dyes, animal or plant-based dyes were used for dyeing (Kocaokutgen et al., 2005). Although natural dyes are a safer and more environmentally friendly option, they are quite costly, more difficult to apply and more difficult to procure. For this reason, the use of natural dyes has not been accepted as practical for many commercial applications. The first artificial dye was discovered by chance in 1886 by Sir William Perkin and was called Mauwein in those years. After this date, dozens of dyes have been synthesized and have been included in the Colour Index since 1925 (Gur et al, 2005, Awale et al, 2013). The classification of dyes can be done from two different perspectives.

[1]Assoc. Prof. Dr. , Adıyaman Üniversity, Vocational School of Technical Sciences, Orcid: 0009-0002-4724-569X

The first of these perspectives is the classification of dyes according to their chemical structures, and the second is the classification of dyes according to their application methods. One of the most important groups of dyes is azo dyes. These dyes contain azo group as chromophore group in their structure. Azo group is -N=N- group and it is the chromophore group with the highest molar absorption values. Azo dyes are prepared as a result of two consecutive reactions called diazotization reaction and then addition reaction. Azo dyes are included in many classes in the classification of dyes according to the application method. Azo dyes are the class with the highest number of dye types among the dye classes. Among the different dye categories, azo dyes are considered to be resistant, non-biodegradable and permanent (Adedayo et al. 2004, Saratale et al. 2011). Synthetic dyes such as azo dyes have become the primary coloring agent in industries such as food, cosmetics and textile industries because trace amounts of dyeing material already produce an intense color (Saratale, et al., 2009, Shah, 2014, Corso, et al., 2009, Alhassani, et al., 2007, Dhaneshvar, et al., 2007). The feature of the present investigation is to synthesize new heterocyclic azo dyes and their polymers. It has been proven that the desired result compounds are obtained by performing structural analysis of all synthesized monomers and polymers. Additionally, the heat resistance of azo compounds was investigated and comparisons were made using the obtained data.

MATERİALS AND METHODS

All compounds used in the synthesis of azo dye compounds (ethyl 4-amino-1-piperidinecarboxylate, 2,7-Naphthalenediol, 1,6-Naphthalenediol, sodium nitrite ($NaNO_2$, ≥97.0%), hydrochloric acid (HCl, 37%), Potassium hydroxide (KOH, ≥85%), Hydrogen peroxide (H_2O_2, 37%)) was purchased from Sigma-Aldrich.

Different analysis techniques were used in the characterization of azo dye compounds. Liquid chromatography/mass spectrometry (LC-MS, TSQ Quantis LC-MS/MS) was used for the determination of the molecular weights of monomers and gel permeation chromatography (GPC, Malvern – OmniSEC) was used for the determination of the molecular weight distribution of polymers. Fourier transform infrared spectroscopy (FTIR, Perkin Elmer Spectrum Two) and nuclear magnetic resonance spectroscopy (NMR, Bruker Avance III HD 600 MHz) analysis techniques were used for the structural analysis of the compounds. Ultraviolet and visible light (UV-Vis, Perkin Elmer Lambda 35) absorption spectroscopy was used to measure the amount of light absorbed or transmitted by azo dye compounds at different wavelengths of light. Also, scanning electron microscopy (SEM, JEOL JSM 5600) was used to obtain information about the topography and composition of the surface of the compounds. Finally, thermogravimetric analysis was performed to investigate the thermal stability of Azo dye compounds (TGA, Hitachi & 7300).

General procedure for the synthesis of novel naphthol based azo dyes (Na1 and Na2)

Heterocyclic azo dye monomers Na1 and Na2 were synthesized by the diazotization-coupling reaction shown in Figure 1. Ethyl 4-amino-1-piperidinecarboxylate (7 mmol) was diazotized using sodium nitrite solution (7 mmol+4 mL H_2O) in the presence of HCl (1 mL HCl+10 mL H_2O). During the diazonium salt production process, an ice bath was used to ensure that the temperature of the reaction medium was below 5 °C. After the mixture was stirred for 1 h, 2,7-Naphthalenediol (7 mmol) in sodium hydroxide solution (7 mmol+10 mL H_2O) was added to the mixture. After the final mixture was stirred for 1 h, the resulting azo dye was filtered. Impurities were removed by washing several times with pure water. The obtained Na1 was dried in an oven. 1,6-Naphthalenediol was used as the

coupling compound in the synthesis of Na2. The yield of Na1 is 75% and the yield of Na2 is 71%.

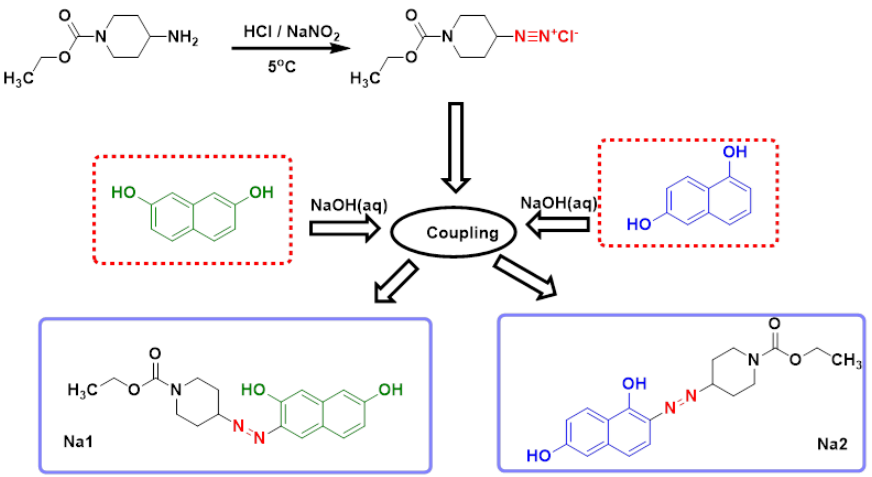

Figure 1. *The synthetic route of azo monomer Na1 and Na2*

General procedure for the synthesis of novel azo dye polymers (PNa1 and PNa2)

The oxidative polycondensation method was used in the synthesis of azo dye polymers. Monomers (5 mmol) were added to a flask containing KOH solution (5 mmol + 20 ml H_2O). The resulting solution was stirred at 70 °C for 30 minutes and then the temperature was increased to 90 °C. At this temperature, H_2O_2 (0.6 ml) was added dropwise to the mixture. After the oxidant addition process, the final mixture was stirred for 8 hours. At the end of the period, the balloon was removed from the reflux and waited for a while to reach room temperature. HCl (37%, 0.5 ml, 0.04 mol) was added to the flask to ensure the precipitation of the formed polymers. The precipitated polymers were filtered and washed with pure water. PNa1 and PNa2 were dried in an oven. The yields of PNa1 and PNa2 are 52% and 57%, respectively.

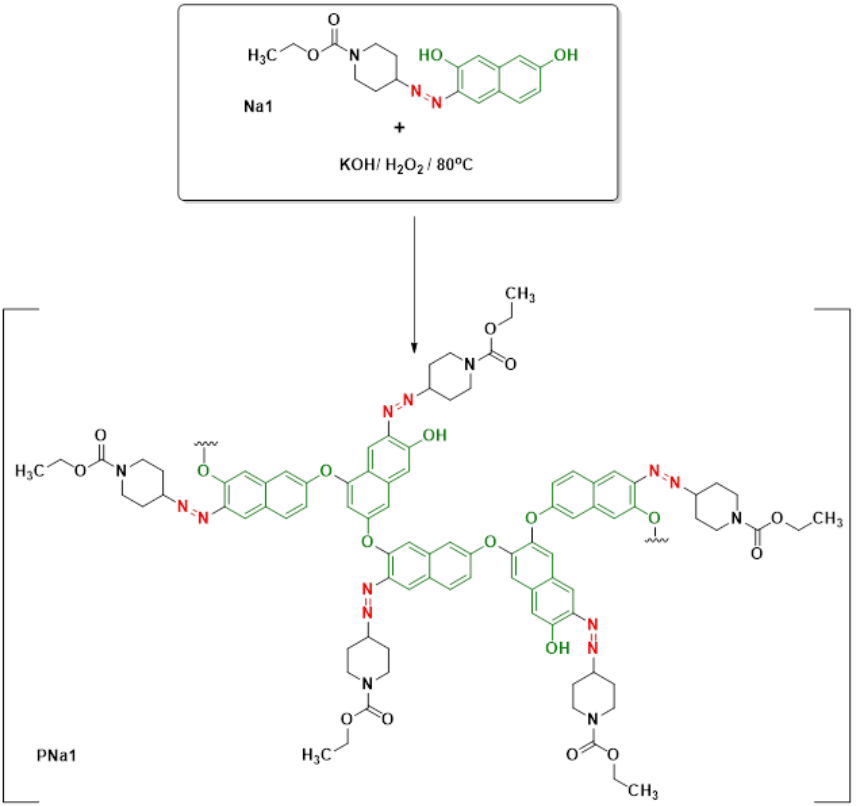

Figure 2. *The synthetic route of azo polymer PNa1 and PNa2*

Thermodynamic and kinetic studies

TGA, DTA and DTG curves were obtained in the temperature range of 20-1000 to determine the thermodynamic parameters. Activation energy (Ea), enthalpy (ΔH), Gibbs free energy (ΔG) and entropies (ΔS) of azo dye monomers and polymers were calculated using the equations of Horowitz and Metzger (Eq.1), Coats-Redfern (Eq.2) and Broido (Eq.3). The equations used are as follows:

Horowitz-Metzger method:

$$Log[f(\alpha)] = \frac{E\theta}{2.303RT_m^2} \quad (1)$$

Coats-Redfern method:

$$\log(\frac{-\ln(1-\alpha)}{T^2}) = \log\frac{A.R}{\beta.E} - \frac{Ea}{2.303.R.T} \quad (2)$$

Broido method:

$$ln[f(\alpha)] = ln\left[\frac{A}{\beta}\left(\frac{R}{E}\right)T_m^2\right] - \frac{E}{RT} \quad (3)$$

Equations 4-6 were used in all methods for the calculation of Enthalpy (ΔH), Entropy (ΔS) and Gibbs free energy (ΔG).

$$\Delta H = E - RT_m \quad (4)$$

$$\Delta G = \Delta H - \Delta S T_m \quad (5)$$

$$\Delta S = 2.303\mathrm{R}\left(\frac{Ah}{kT_m}\right) \quad (6)$$

RESULTS AND DİSCUSSİON

LC-MS / GPC

In the LC-MS technique, sample molecules separated according to their physicochemical properties are analyzed with a mass detector. Mass spectrometers convert molecules into charged ionized molecules by exciting them with the ionization process. As a result of the LC-MS analysis of Na1 and Na2, it was determined that the molecular ion values (m/z) were 343. The GPC chromatograms of PNa1 and PNa2 polymers were obtained to determine the mass average molecular weight (Mn), mass average molecular weight (Mw) and polydispersity index (PDI) values. The values obtained from the GPC chromatogram of PNa1 and PNa2 were Mn: 4.387 and 4.699 g mol^{-1}, Mw: 4458 and 4876 g mol^{-1}, PDI: 1.01 and 1.03, respectively.

FT-IR Spectroscopy

FT-IR spectra of the azo monomers and polymers were recorded as KBr pellets in the region 4000–400 cm^{-1}. Bands confirming the main structure of the compounds can be clearly seen in the FTIR spectra of the compounds (Fig.3 and 4). In the spectrum

of Na1, absorption bands appeared in the 3441–3283 cm^{-1} areas, which were attributed to naphthol OH groups (Fig.3).

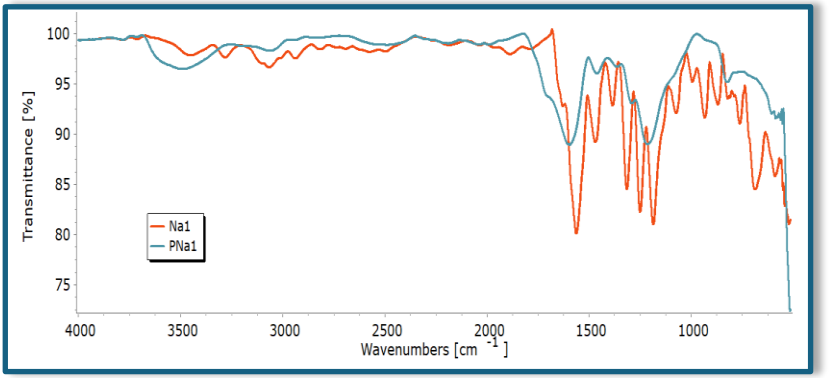

Figure 3. *The FT-IR spectrum of Na1 and PNa1*

The aromatic C–H stretching vibrations appeared as two weak bands at 3058–2939 cm^{-1}. Also, two weak bands seen at 1884 and 1794 cm^{-1} were formed as a result of carbonyl stretching vibration. The presence of alkyl groups is generally understood by the C-H stretching vibration bands seen from weak to strong in the 2850-2990 cm^{-1} region. It also gives C-H bending vibration bands in the 1375 and 1450 cm^{-1} region. Ethyl attached to the ester group C-H stretching vibration bands were formed at 2818 cm^{-1}, and bending vibration band was formed at 1386 cm^{-1}. A high intensity band is observed at 1574 cm^{-1} due to the presence of the aromatic C=C. The medium band at 1475 cm^{-1} seen in the spectrum indicates the presence of the azo group.

In the spectrum of Na2, bands were formed in a similar region to the spectrum of Na1. This is because the main structures of Na2 and Na1 are the same. (Fig.4) The medium bands observed at 3454 and 3282 cm^{-1}, small bands at 3066 and 2937 cm^{-1} and weak bands at 2818 and 2706 cm^{-1} can be attributed to naphthol OH, aromatic C-H and aliphatic C-H stretching vibrations, respectively. The weak band appeared at 1893 cm^{-1} due to the carbonyl stretching

vibration. A strong band originating from aromatic C=C stretching was observed at 1565 cm−1. In addition, N=N stretching vibration band occurred at 1473 cm−1.

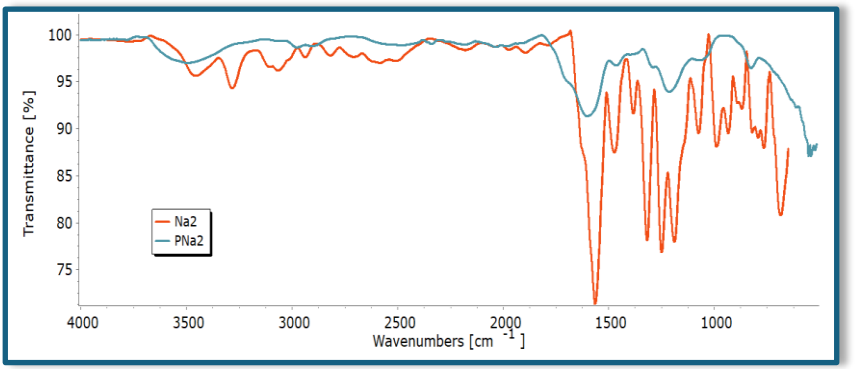

Figure 4. *The FT-IR spectrum of Na2 and PNa2*

In the spectrum of polymers, bands that support polymer formation have been formed. Polymers are molecules with high molecular weights formed by the combination of more than one monomer. Therefore, there are repeating units in their main structure. Bands are formed at the same wavelengths as a result of similar vibrations of more than one monomer atom. This is the reason why PNa1 and PNa2 form fewer and wider bands in their spectrums than their monomers. The medium broad band at 3494 cm^{-1} in the spectrum of PNa1 was formed as a result of the OH stretching vibration that did not participate in the polymer formation. The bands due to OH stretching vibration at 3484 cm^{-1} are observed for PNa2. Aromatic and aliphatic C-H stretching vibrations combined to form weak bands at 3062 cm^{-1} for PNa1 and in the range of 2976-2904 cm^{-1} for PNa2. The C=C and C=O stretching vibration bands overlapping to form a broad band at 1596 cm^{-1}. The broad band belonging to these groups is at 1602 cm-1 for PNa2. The weak bands occurring at 1461 cm^{-1} in the spectrum of PNa1 and at 1464 cm^{-1} in the spectrum of PNa2 belong to N=N stretching vibrations.

^{1}H NMR Spectral data

In the ^{1}H-NMR spectrum of azo dye monomer and polymers taken in DMSO-d_6, all peaks that illuminate the structures of the compounds are present. In the ^{1}H-NMR spectrum of Na1, OH proton peaks are observed at 13.36 and 10.69 ppm. Peaks formed in the range of 7.88-6.47 ppm belong to aromatic ring protons. Ethyl protons attached to the ester group formed a peak at 2.51 ppm. The peak observed at 1.19 ppm proves the presence of cyclic aliphatic protons. Since the main structure of Na2 is similar to Na1, peaks were formed in the same regions in their spectra. In the spectrum of Na2, it is seen that OH, aromatic ring and methyl protons have the same chemical shifts as Na1. Only aliphatic protons were formed two different peaks at 1.19 and 1.14 ppm with different intensities.

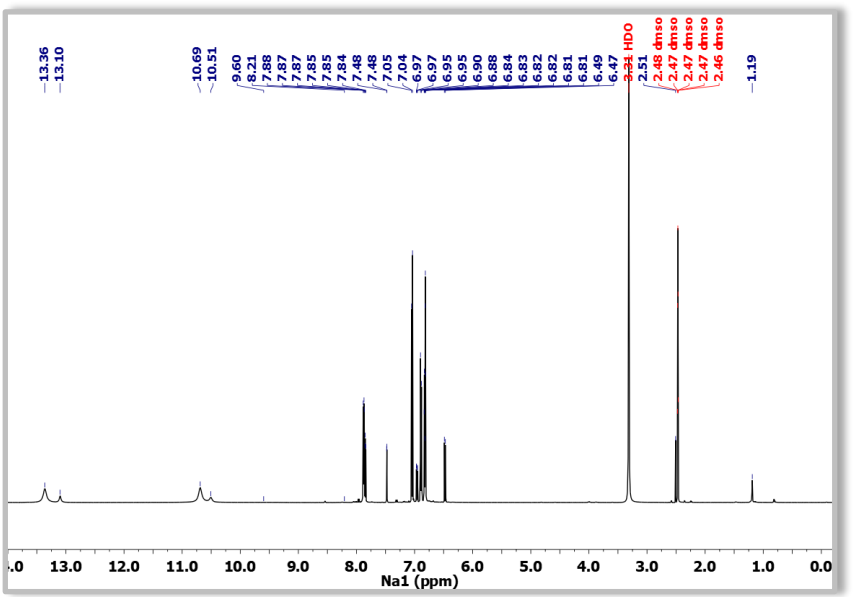

Figure 5. *^{1}H-NMR spectrum of azo monomer Na1*

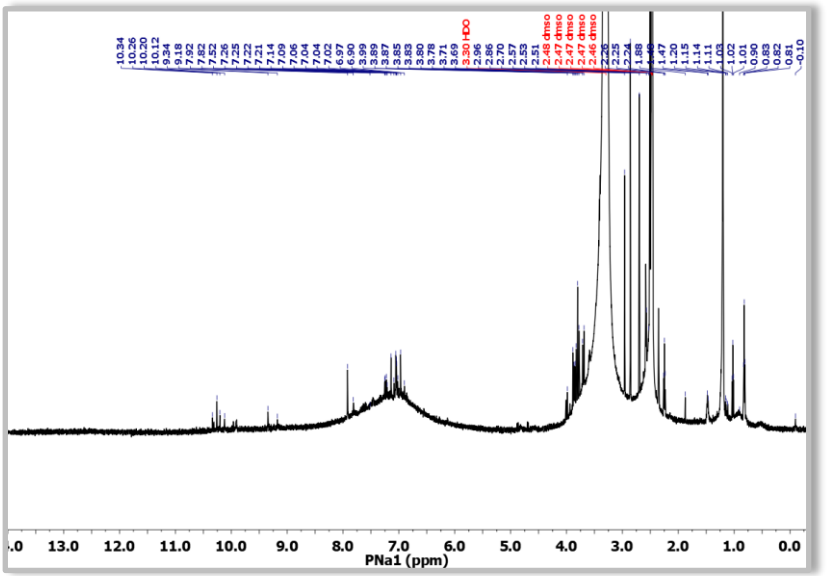

Figure 6. *^{1}H-NMR spectrum of azo polymer PNa1*

There are peaks supporting polymer formation in the spectra of PNa1 and PNa2. Especially the formation of aromatic and aliphatic ring protons in the form of hill is evidence that polymer formation has occurred. A similar situation is valid for ethyl protons. Aromatic ring proton peaks formed a hill appearance in the spectra of both polymers. This is because many peaks formed in the same region. OH protons that do not participate in polymer formation formed peaks at different points in both spectra. These peaks formed in the range of 10.34-9.18 ppm in the spectrum of PNa1 and in the range of 10.14-9.95 ppm in the spectrum of PNa2. The aromatic ring proton peaks for PNa1 and PNa2 occurred in the range of 7.92-6.90 ppm and 7.92-7.00 ppm, respectively. The numerous peaks with different intensities occurring in the range of 3.99-2.24 ppm and 4.89-2.23 ppm belong to the ethyl proton of PNa1 and PNa2, respectively. Aliphatic ring protons formed numerous peaks in the range of 1.88-0.81 ppm for PNa1 and 1.88-0.79 ppm for PNa2.

Electronic Spectra

UV-vis spectra of azo dye monomer and polymers were investigated in three different solvents (DMF, DMSO and Ethanol).The data obtained from UV-vis spectra are shown in the table 1. In UV-vis spectroscopy of organic compounds, electronic transitions are generally based on the transition of n or π electrons to the π* excited state; the energies required for these processes ensure that the absorption peaks are in the appropriate spectral region (200-700 nm). Monomers and polymers have formed absorption bands at different wavelengths and intensities depending on the solvent type. In the spectrum of Na1, 5 bands belonging to different electronic transitions are seen. The bands seen in the range of 307-231 nm are formed as a result of π-π* transitions belonging to the naphthol ring (Fig.7). The π-π* electronic transition of the C=O group only formed a band at 368 nm in DMF solvent. This situation clearly shows the effect of the solvent on the absorption properties of the compounds. The absorption bands at 425 nm (in Ethanol), 431 nm (in DMSO) and 439 nm (in DMF) are formed as a result of π-π* electronic transitions between the azo group and the naphthol ring system. The spectra of Na2 contain absorption bands that are quite different from the spectrum of Na1 (Fig.8). While two bands were formed in the spectrum of Na2 in DMSO, three bands were formed in the spectra in DMF and ethanol. The absorption bands occurring at 272 and 397 nm in the spectrum in DMSO belong to the π-π* electronic transitions of the naphthol ring and C=O group, respectively. In the spectrum in DMF, the bands belonging to the π-π* electronic transitions of the naphthol ring and C=O group were formed at 239 and 374 nm, respectively. In the spectrum in ethanol, the π-π* electronic transition band of the C=O group was not formed.

Table 1. *UV–vis spectrum data of azo dye monomers and polymers in DMF, DMSO and Ethanol*

Compound	Solvent	A	B	C	D	E	
		λ_{max}[a]	λ_{max}[a]	λ_{max}[a]	λ_{max}[a]	λ_{max}[a]	ε_{max}[b]
Na1	DMF	232	307	368	439	-	-
	DMSO	246	291	-	431	-	-
	Ethanol	231	295	-	425	-	-
PNa1	DMF	-	294	318	-	661	16
	DMSO	249	300	363	-	662	11
	Ethanol	-	302	365	-	-	-
Na2	DMF	239	-	374	472	-	-
	DMSO	-	272	397	-	-	-
	Ethanol	228	300	-	430	-	-
PNa2	DMF	-	304	399	485	-	-
	DMSO	242	320	399	498	548	226
	Ethanol	-	293	367	-	-	-

a:The wavelength of the band (nm); b: molar absorptivity coefcient (mol^{-1} l cm^{-1})

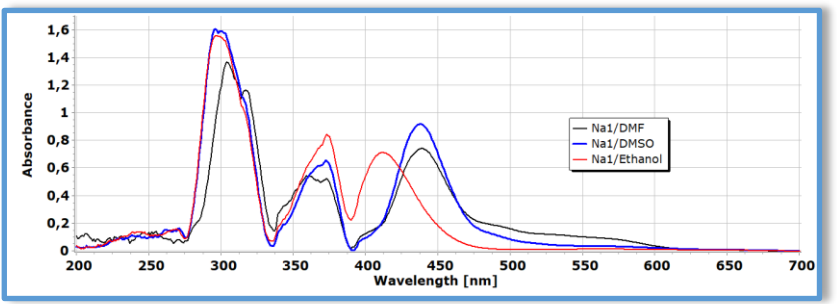

Figure 7. *UV-Vis spectra of azo monomer Na1 in DMSO, DMF and ethanol*

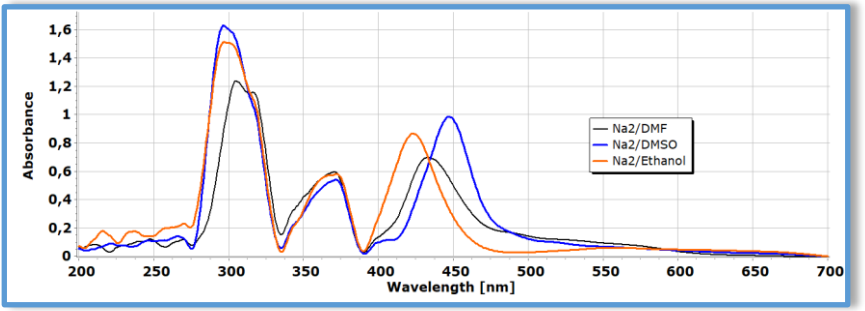

Figure 8. *UV-Vis spectra of azo monomer Na2 in DMSO, DMF and ethanol*

The naphthol ring absorption bands formed at 228 and 300 nm. In the UV-vis spectra of polymers, bands that are not present in the spectra of monomers are observed. These bands, which occur above 500 nm, are formed as a result of charge transfer transitions. Some organic compounds form organic electron donors and acceptors in the solvent they are in. Several organic charge transfer complex systems have been developed that are weakly associated with these compounds. PNa1 formed a charge transfer transition band at 661 and 662 nm in its spectra in DMF and DMSO, respectively (Fig.9).

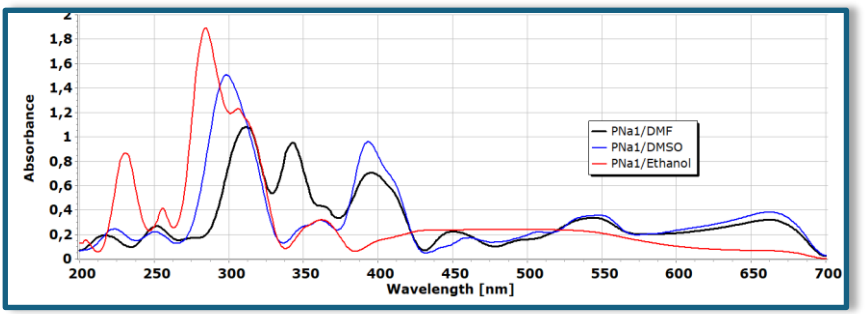

Figure 9. *UV-Vis spectra of azo monomer PNa1 in DMSO, DMF and ethanol*

PNa2 formed a CT band at 548 nm only in DMSO (Fig.10). The electronic transition bands of the naphthol ring and C=O group of PNa1 occurred in the ranges of 249-302 nm and 318-365 nm,

respectively. In PNa2, these bands are seen in the range of 242-293 nm and 367-399 nm, respectively. One of the biggest differences seen in the spectra of PNa1 and PNa2 is They are π-π* electronic transitions between the azo group and the naphthol ring system. This band did not occur in any of the spectra of PNa1. In the spectra of PNa2, bands were formed at 485 and 498 nm in DMF and DMSO, respectively.

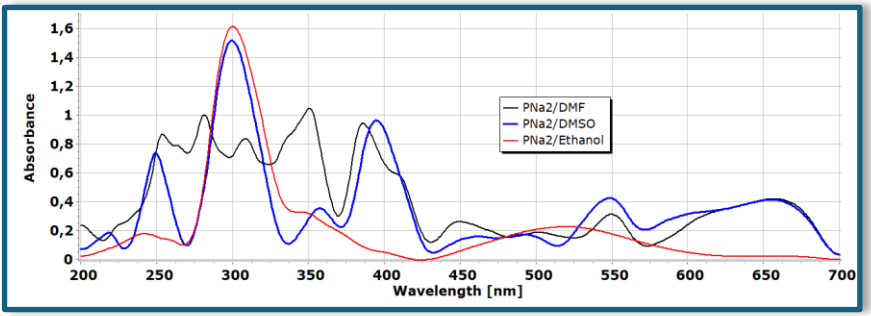

***Figure 10**. UV-Vis spectra of azo monomer PNa2 in DMSO, DMF and ethanol*

SEM analyses

SEM analyses were performed to investigate the surface morphologies of the synthesized azo dye monomers and polymers and the images obtained are given in Figur 11-14. In SEM analyses, different information about the examined sample can be obtained from various signals. In Figure 11 SEM images of Na1 are given; it can be seen that it gives rock-like appearances in different sizes.

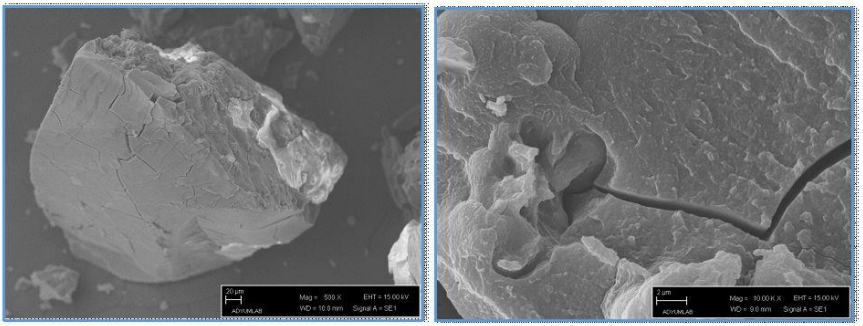

Figure 1. *Scanning electron micrographs (SEM) image of azo monomers Na1*

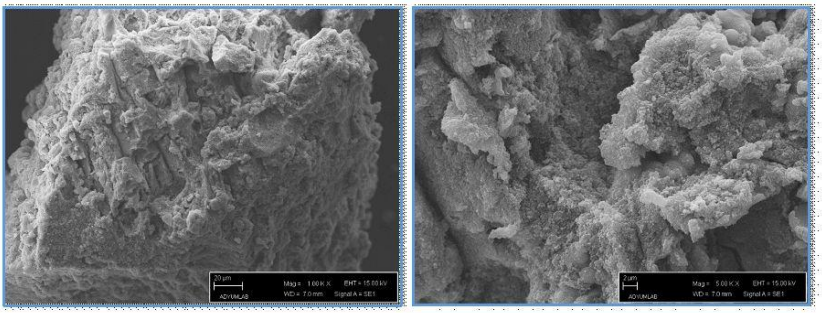

Figure 12. *Scanning electron micrographs (SEM) image of azo monomers PNa1*

This situation shows that Na1 does not have a standard morphology, that is, it is amorphous. Similar appearances are found in SEM images of Na2 (Fig.13). It is seen that both Na1 and Na2 have a layered structure and the number of pores is less. SEM images of polymers clearly present morphological changes proving that polymerization has occurred. The morphologies of PNa1 and PNa2 are quite different from their monomers. Especially PNa1 has been a more layered and porous structure after polymerization. PNa2, unlike PNa1, has been a decreased layered structure and pore number.

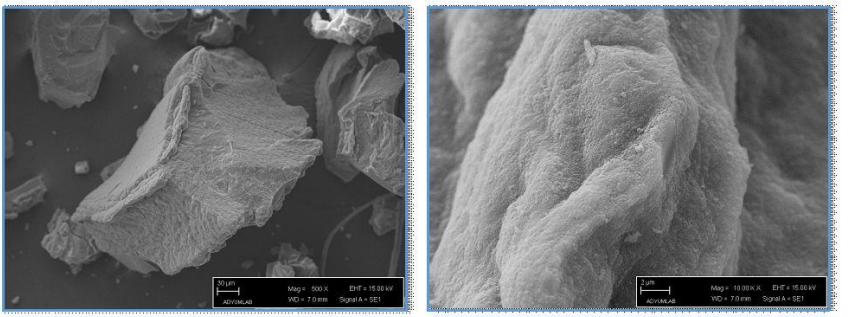

Figure 13. *Scanning electron micrographs (SEM) image of azo monomers Na2*

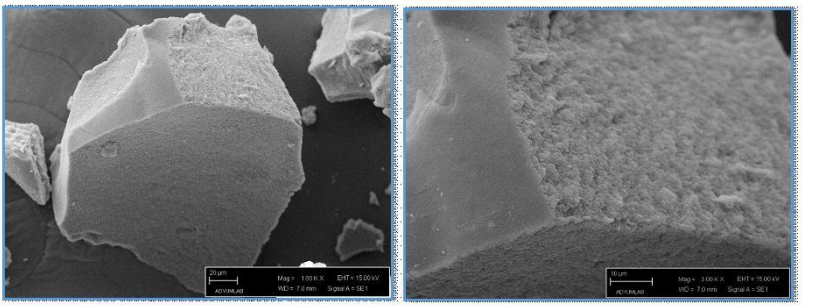

Figure 14. *Scanning electron micrographs (SEM) image of azo monomers PNa2*

Thermogravimetry of Polyazo Dyes

Thermal analysis is a group of methods in which the physical properties of the substance and/or its reaction products are measured as a function of temperature when a controlled temperature program is applied to the substance. TGA analysis was performed to determine the resistance of the synthesized azo dyes and polymers to heat increase. All TGA analyses were performed at 15 heating rates in the temperature range of 20-1000 ℃. Figure 13-16. Thermograms of Na1, Na2, PNa1 and PNa2 are presented. Data obtained from thermogams are given in Table 2 and 3. It is seen in the thermograms of monomers and polymers that there are mass losses at temperatures below 100 ℃. The reason for these mass

losses is water that has formed an extramolecular bond with monomers and polymers. Mass losses in monomers occurred in two steps. The first mass loss of Na1 occurred at 136 ℃, while the first mass loss of Na2 occurred at 226 ℃. There is a significant difference between the temperatures at which the initial mass losses of Na1 and Na2 occur. The reason for this difference is that Na2 has formed a dimeric structure. In addition, when the remaining amounts of matter are compared as a result of the analysis, it is seen that Na2 has the largest value (62.43%).

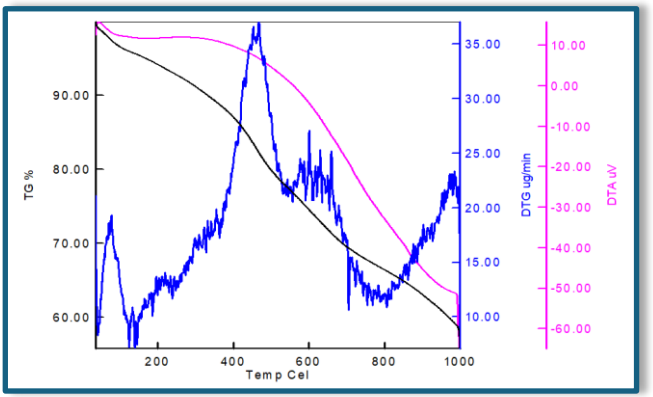

Figure 15. *TG, DTG and DTA curves of azo monomer Na1*

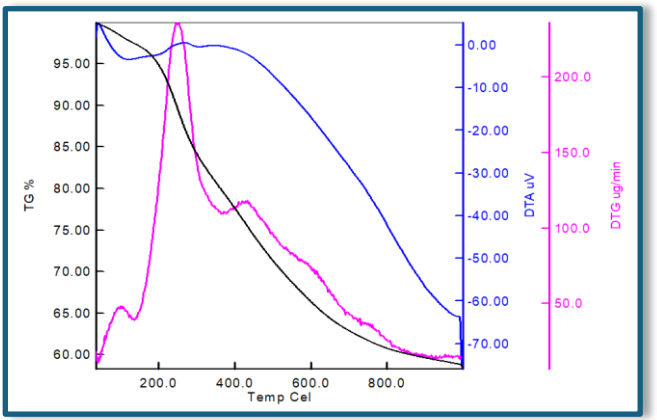

Figure 16. *TG, DTG and DTA curves of azo polymer PNa1*

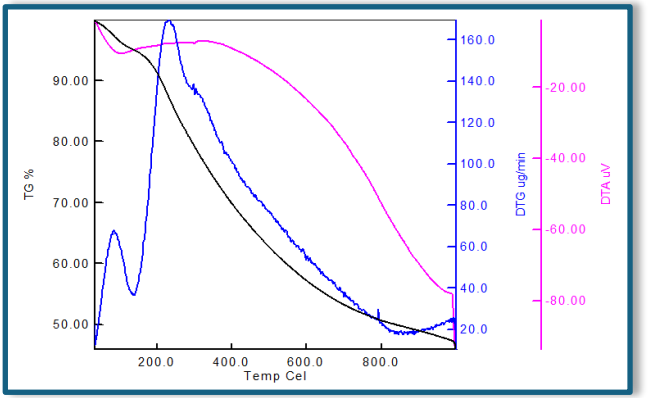

Figure 17. *TG, DTG and DTA curves of azo monomer Na2*

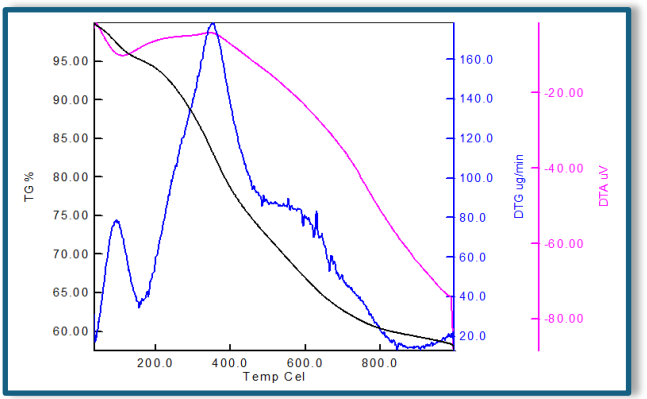

Figure 18. *TG, DTG and DTA curves of azo monomer PNa2*

Estimation of thermodynamic parameters

Any characteristic of a system or substance is called a property. Some of the frequently encountered properties in thermodynamics are activation energy (Ea), enthalpy (ΔH), Gibbs free energy (ΔG) and entropy (ΔS). The thermodynamic parameters obtained from the calculations made using the Horowitz and Metzger, Coats-Redfern and Broido methods of the synthesized monomers and polymers are presented in the table 4-7. Activation energy (Ea) is the energy value that must be overcome for a chemical

reaction to occur. The data obtained as a result of the calculations show that the Ea of the thermal decomposition steps of all the synthesized compounds are different from each other. This result revealed that the resistance of the compounds to temperature increase is different. The highest Ea belongs to Na2 in monomers and PNa2 in polymers. Although the main structures of the monomers are similar, the different docking points give the compounds different chemical properties. Therefore, the polymers synthesized from these monomers have different chemical properties. In addition, the amounts of oligomers with different chain lengths in polymers affect the thermal stability of polymers.

The enthalpies (ΔH) of azo dye monomers and polymers show the sum of all kinds of energy in the environment during thermal degradation. Thermal degradation reactions are mostly endothermic reactions. Therefore, extra energy must be given to the environment for structural degradation to occur. When the ΔH of monomers is compared, the highest enthalpy belongs to the first step of the Na2 monomer. It is seen that the ΔH of PNa2 in polymers is higher than PNa1. This result is evidence that the thermal stability of Na2 in monomers and PNa2 in polymers is high.

Table 2. *Thermal stability and thermal degradation data of synthesızed monomers and polymers*

Compound	β	T_i	T_{25}	T_{50}	T_{75}	T_f	Residue%
Na1	**15**	**136**	**439**	**-**	**-**	**1000**	**58.26**
Na2	**15**	**226**	**614**	**-**	**-**	**1000**	**62.43**
PNa1	**15**	**158**	**452**	**-**	**-**	**1000**	**57.48**
PNa2	**15**	**131**	**488**	**-**	**-**	**1000**	**51.34**

Ti : İnitial decomposition temperature, T25, 50, 75: Temperature for 25, 50, 75% weight loss, Tf : end of decomposition experiment

Table 3. *TG-DTA characteristic parameters of synthesized monomers and polymers*

Compound	β	1st			2nd		
		T_a	T_b	%c	T_a	T_b	%c
Na1	15	136-360	248	17.22	372-544	430	10.32
Na2	15	226-381	355	4.494	381-845	569	21.25
PNa1	15	158-503	352	23.08	-	-	-
PNa2	15	131-847	510	39.40	-	-	-

Ta: Mass loss temperature ranges, Tb: Maximum temperature on the DTA curve, %c: Percentage of lost mass of the sample in the temperature range

The ΔG of the synthesized compounds is positive. In cases where ΔG > 0, energy must be given from the outside to the environment for thermal degradation to continue. The energy given to the environment moves the degradation reaction in the direction of products. The ΔG of the second thermal decomposition steps of monomers is higher than the ΔG of the first thermal decomposition steps. In polymers, the ΔG of PNa2 is higher than the ΔG of PNa1

Table 4. *Activation energy of synthesızed monomers and polymer*

Compound	Stage	Horowitz/Metzger	Coats-Redfern	Broido
		Ea (kj.mol^{-1})	Ea (kj.mol^{-1})	Ea (kj.mol^{-1})
Na1	Stg1st	58.6	8.79	71.1
	Stg2nd	2.05	26.3	116
Na2	Stg1st	194	14.2	88.5
	Stg2nd	6.48	57.1	183
PNa1	Stg1st	2.59	14.1	76.6
PNa2	Stg1st	20.3	42.4	159

Table 5. *Kinetic parameters of synthesızed monomers and polymers using Horowitz-Metzger equation.*

Compound	Stage	A (min^{-1})	ΔH ($kj.mol^{-1}$)	-ΔS ($kj.mol^{-1}$)	ΔG ($kj.mol^{-1}$)
Na1	$Stg1^{st}$	$1.12x10^{4}$	54.35	$171x10^{-3}$	143
	$Stg2^{nd}$	$2.76x10^{3}$	3.780	$185x10^{-3}$	126
Na2	$Stg1^{st}$	$9.06x10^{5}$	189.5	$136x10^{-3}$	275
	$Stg2^{nd}$	$2.34x10^{4}$	0.504	$169x10^{-3}$	142
PNa1	$Stg1^{st}$	$2.18x10^{3}$	2.589	$186x10^{-3}$	114
PNa2	$Stg1^{st}$	$1.54x10^{4}$	13.88	$172x10^{-3}$	148

In thermal decomposition reactions, the increase in the temperature of the environment over time caused the ΔS of the environment to increase. The data obtained from the calculations show that the ΔS are negative. This result shows that the thermal decomposition process of the compounds becomes easier with the increase in temperature. The highest ΔS belongs to Na2 (-ΔS Horowitz and Metzger: 136x10-3 $kj.mol^{-1}$, -ΔS Coats-Redfern: 151x10-3 $kj.mol^{-1}$ and -ΔS Broido: 0.48x10-3 $kj.mol^{-1}$).

Table 6. *Kinetic parameters of synthesızed monomers and polymers using Coats-Redfern equation.*

Compound	Stage	A (min^{-1})	ΔH ($kj.mol^{-1}$)	-ΔS ($kj.mol^{-1}$)	ΔG ($kj.mol^{-1}$)
Na1	$Stg1^{st}$	$1.69x10^{3}$	4.472	$187x10^{-3}$	102
	$Stg2^{nd}$	$3.54x10^{4}$	20.50	$164x10^{-3}$	136
Na2	$Stg1^{st}$	$6.65x10^{4}$	9.079	$158x10^{-3}$	108
	$Stg2^{nd}$	$2.06x10^{5}$	50.15	$151x10^{-3}$	177
PNa1	$Stg1^{st}$	$1.18x10^{4}$	8.942	$172x10^{-3}$	116
PNa2	$Stg1^{st}$	$3.21x10^{4}$	35.92	$166x10^{-3}$	166

Table 7. *Kinetic parameters of synthesized monomers and polymers using Broido equation.*

Compound	Stage	A (min^{-1})	ΔH ($kj.mol^{-1}$)	-ΔS ($kj.mol^{-1}$)	ΔG ($kj.mol^{-1}$)
Na1	$Stg1^{st}$	$3.20x10^{6}$	66.85	$124\ x10^{-3}$	131
	$Stg2^{nd}$	$1.16x10^{8}$	110.8	$0.97x10^{-3}$	179
Na2	$Stg1^{st}$	$5.52x10^{6}$	83.30	$121x10^{-3}$	159
	$Stg2^{nd}$	$5.25x10^{8}$	176.0	$0.48x10^{-3}$	216
PNa1	$Stg1^{st}$	$6.10x10^{5}$	71.44	$140x10^{-3}$	159
PNa2	$Stg1^{st}$	$1.13x10^{10}$	152.5	$0.60x10^{-1}$	199

CONCLUSİON

Heterocyclic azo dyes constitute a large part of the dyes used in the food, cosmetics, paper, textile and leather industries today. Researchers continue to synthesize new azo dyes using different starting materials. In this study, two azo dye polymers with different molecular weights that were not found in the literature were synthesized. Naphthol-derived azo dye monomers were used in the synthesis of polymers. The absorption properties of azo monomers and polymers vary depending on the solvent used. There are bathochromic and hypsochromic shifts in the bands due to the interaction of the compounds with the solvent in the spectra. In addition, as a result of the polymerization of monomers, compounds with different thermal stability were formed and therefore each compound brought about different thermal decomposition curves. This result shows that even if the main structure of the compounds is similar, even very small differences in the structure cause physical and chemical changes in the compounds.

REFERENCES

Kocaokutgen, H., Gur, M., Soylu, S., Lonnecke P. (2005). Spectroscopic, thermal and crystal structure properties of novel (E)-2,6-dimethyl-4-(4-tert-butylphenyldiazenyl)phenyl acrylate dye *Dyes Pigm*., 67(2), 99-103.

Awale, A.G., Gholse, S.B., Utale, P.S. (2013). Synthesis, spectral properties and applications of some mordant and disperse mono azo dyes derived from 2-amino-1, 3-benzothiazole. *Res. J. Chem. Sci.* 3(10), 81-87.

Adedayo, O., Javadpour, S., Taylor, C., Anderson, W.A., Moo-Young, M. (2004). Decolorization and Detoxification of Methyl Red by aerobic bacteria from a wastewater treatment plant. *World J Microbiol Biotechnol.* 20(6), 545-550.

Saratale, R.G., Saratale, G.D., Chang, J.S., Govindwar, S.P. (2011) Bacterial decolorization and degradation of azo dyes: a review. *J. Taiwan Inst. Chem. Eng.* 42(1), 138-157.

Saratale, R.G., Saratale, G.D., Kalyani, D.C., Chang, J.S., Govindwar, S.P. (2009) Enhanced decolorization and biodegradation of textile azo dye Scarlet R by using developed microbial consortium-GR. *Bioresour Technol* 100(9), 2493-2500.

Shah, K. (2014) Biodegradation of azo dye compounds. *Int. Res. J. Biochem. Biotech* 1(2), 005-013.

Corso, C.R., Maganha De Almeida, A.C. (2009) Bioremediation of dyes in textile effluents by Aspergillus oryzae. *Microb. Ecol.* 57(2), 384-390.

Alhassani, H. A., Rauf, M. A., Ashraf, S. S. (2007). Efficient microbial degradation of toluidine blue dye by Brevibacillus sp. *Dyes and Pigments*, 75(2), 395-400.

Dhaneshvar, N.;Ayazloo, M.;Khatae A.R. and Pourhassan M., 2007. Biological decolourization of dye solution containing malachite green by microalgae cosmarium sp. *Bioresource Technology*. 143(1), 214-9.

KİMYA BİLİMİNDE DİSİPLİNLERARASI YAKLAŞIMLAR